Redox interactions in cytochrome c oxidase: from the "neoclassical" toward "modern" models

Richard W. Hendler and Hans V. Westerhoff*

Laboratory of Cell Biology, National Heart, Lung, and Blood Institute, National Institutes of Health, Bethesda, Maryland 20892 USA; and *E. C. Slater Institute for Biochemical Research, University of Amsterdam, and Division of Molecular Biology, Netherlands Cancer Institute, 1066 CX Amsterdam, The Netherlands

ABSTRACT Because of recent experimental data on the redox characteristics of cytochrome *c* oxidase and renewed interest in the role of cooperativity in energy coupling, the question of redox cooperativity in cytochrome *c* oxidase is reexamined. Extensive redox cooperativity between more than two redox centers, some of which are spectrally invisible, may be expected for this electron transfer coupled proton pump. Such cooperativity, however, cannot be revealed by the traditional potentiometric experiments based on a difference in absorbance between two wavelengths. Multiwavelength analyses utilizing singular value decomposition and second derivatives of absorbance vs. wavelength have revealed a stronger cooperativity than consistent with the "neoclassical" model, which allowed only for weak negative cooperativity between two equipotential one-electron centers. A thermodynamic analysis of redox cooperativity is developed, which includes the possibilities of strong cooperative redox interactions, the involvement of invisible redox centers, conformational changes, and monomer/dimer equilibrations. The experimental observation of an oxidation of one of the cytochromes (a_3) with a decrease in applied redox potential is shown to require both strong negative cooperativity and the participation of more than two one-electron centers. A number of "modern" models are developed using the analytical approaches described in this paper. By testing with experimental data, some of these models are falsified, whereas some are retained with suggestions for further testing.

INTRODUCTION

Cytochrome oxidase (aa_3) is an amazingly complex enzyme. As isolated in the dimer form, it contains 4 Fe, 5–6 Cu, 2 Zn, and 2 Mg (Einarsdóttir and Caughey, 1984, 1985*a, b;* Bombelka et al., 1986; Steffens et al., 1987). There are 9–10 redox active metal centers per unit dimer (i.e., the Fe and Cu centers). Both monomers and dimers show enzyme activity. Equilibration between the two forms could be important in the control of activity. The enzyme is asymmetrically oriented in energy transducing membranes where it coordinates the flow of four electrons and four protons to O_2 forming 2 H_2O. Simultaneously, it pumps additional protons from the interior of a vesicle (i.e., mitochondrion or bacterium) to the outside, forming an electrochemical potential for protons, which captures a major fraction of the free energy liberated in the redox reactions (Wikström et al., 1981). These activities may use major conformational changes in the enzyme. As witnessed in the case of hemoglobin, proteins are able to coordinate processes in subtle ways. The binding of one ligand can alter the affinity of the protein for a second ligand. Cooperative interactions of this type may enhance catalysis, improve regulatory properties, and even be at the origin of energy coupling by enzymes (Hill, 1985; Kamp et al., 1988). The possibilities and probabilities for such cooperative interactions in the binding of ligands of a single type (i.e., electron–electron; electrons may be considered as ligands, see below) or of different types (i.e., proton–electron) and the influence of conformation and state of aggregation on ligand binding are enormous. Yet, these kinds of interactions barely have been explored.

A model of cooperative interaction involving only two electrons and two heme centers was presented in 1974 (Malmström, 1974; Nicholls and Petersen, 1974). The model was well received and adequate to explain observations that appeared to require some form of cooperativity between the heme centers (see Wikström et al., 1976). In the cytochrome oxidase literature, this model has been referred to as the "neoclassical model." Although the name is somewhat inappropriate, we shall continue to refer to it as such in this review to maintain correspondence with the existing literature.

The purpose of this article is to review the research that led to the development of the simple two electron model for cytochrome oxidase, to show why this model is no longer adequate, and to stimulate the development of "modern" cooperative redox models. In the presentation that follows, experimental potentiometric titration data are "fitted" to a number of discrete hypothetical models that include up to six electrons, two to four redox centers, and changes in conformation and state of aggregation. Although the fittings are sometimes quite successful, it is important to stress at the beginning that we believe it is premature to accept that any of the particular models we have chosen is likely to be the "true model." The reason for trying to extend the cooperative treatment for redox interactions in cytochrome oxidase is that newer findings cannot be explained by the current models. Our main intention is to present an approach that will allow the development and analysis of models that are more appropriate for this sophisticated enzyme. We then show that some of the latter models can account for all of the data now available.

The present article is presented in four parts. In the first part, a brief history is provided to show the origins of our current understandings and confusions. The second part discusses new approaches for studying the thermodynamic properties of cytochrome aa_3 and results obtained

0006-3495/92/12/1586/19 $2.00

by the new methodology. The third part develops the idea that interactions between and among the various redox centers in the molecule involve strong, rather than the previously assumed weak, cooperative influences. The fourth part introduces techniques for constructing and evaluating models that involve strong interactions among all of the centers and considers the influences of conformational and state-of-aggregation changes on the thermodynamic properties of the enzyme.

1. HISTORICAL BACKGROUND FOR CURRENT VIEWS AND CONTROVERSIES CONCERNING REDOX COOPERATIVITY IN CYTOCHROME c OXIDASE

In a series of papers from 1970 to 1974, Wilson and Dutton and their collaborators laid the foundation for our current views on the redox behavior of the heme centers of cytochrome oxidase (Wilson and Dutton, 1970; Tsudzuki and Wilson, 1971; Wilson et al., 1972; Leigh et al., 1974). Potentiometric titrations were optically monitored at ΔA (605–630 nm), and the enzyme was studied in situ in mitochondria from pigeon heart and rat liver, as well as in isolation. The essential result was that heme *a* and heme a_3, each titrated individually as $n = 1$ centers with E_m values near 220 and 360 mV, respectively, and each center accounted for 50% of the total. Tiesjema et al. (1973) confirmed this picture using purified enzyme from beef heart.

The conclusions of Wilson and his collaborators, however, ran counter to other information regarding the spectral properties of the two heme centers. It generally has been accepted that although both hemes contribute equally to the Soret absorbance near 445 nm, heme *a* accounts for >80% of the total ΔA (605–630 nm) and heme a_3 for <20%. Experimental support for this view goes back >30 years when Yonetani (1960*a, b*) used a series of difference spectra from differently treated preparations of cytochrome oxidase to deduce the individual reduced minus oxidized difference spectra for cytochromes *a* and a_3. Studies by Vanneste (1966) and Horie and Morrison (1963) led to essentially similar results. It is important to note, however, that the conclusions of all of these studies rest on important assumptions that were both explicit and implicit, namely:

(*a*) The addition of a ligand (including an electron) to one redox center will have no effect on the spectrum or redox state of the other center.

(*b*) The presence of CN^- locks heme a_3 in the oxidized state, so that added reductants will cause the reduction of only heme *a*. Similarly, the presence of CO locks heme a_3 in the reduced state, so that added oxidants will oxidize only heme *a*.

(*c*) Combinations of difference spectra using different preparations of CO and HCN liganded enzymes, in different states of reduction for heme *a* and a_3, follow the rules of algebraic addition, and variations due to the use of several different preparations of the enzyme are negligible.

Although the work of Yonetani, Vanneste, and Hori and Morrison gave valuable information as to the relative contributions of cytochromes *a* and a_3 to the Soret and α peaks under certain sets of conditions, the actual isolated spectra deduced for the two cytochromes cannot be accepted without question because of the many assumptions involved in the procedures. For example, the belief that the ligand, CO, can hold cytochrome a_3 in the reduced state has been shown to be incorrect (Sidhu and Hendler, 1990; Hendler, 1991). Neither can it be assumed that each cytochrome will contribute a constant percentage to the absorbance in the Soret and α regions at all voltages (see Caughey et al., 1976; Hendler and Sidhu, 1988) nor that the presence of a ligand on one center will have absolutely no affect on the unliganded center. There is evidence for an allosteric interaction by which the binding of CO or CN^- to cytochrome a_3 does produce conformational changes that affect the spectra attributable to cytochrome *a* (Sherman et al., 1991). Further evidence for allosteric interactions between heme *a* and the binuclear site come from Yoshikawa, Caughey, and co-workers (Yoshikawa and Caughey, 1982, 1992; Yoshikawa et al., 1985; Einarsdóttir et al., 1988). It was found that a change in the redox state of cytochrome *a* affected the stretch frequencies of heme a_3, ligated with either CO, CN^-, or azide.

Returning to the potentiometric titrations of Wilson and his co-workers, how can the ΔA (605–630 nm) show two independent titrations for heme *a* and heme a_3, each accounting for 50% of the total ΔA, when 80% (or more) of this ΔA is due to heme *a*? The answer from Wilson and his collaborators was that in the absence of ligands to heme a_3, each heme does account for 50% of the ΔA. They proposed that there is a form of heme–heme interaction whereby the binding of a ligand to heme a_3 causes an enhancement in the extinction coefficient (∈) of heme *a* at 605 nm (Wilson and Leigh, 1974; Wilson et al., 1972). Therefore, the effect of adding the ligand is not simply the removal or alteration of the absorbance due to heme a_3, but there is a net increase in the absorbance of heme *a* so that the apparent contribution of heme a_3 to the α absorbance becomes underestimated.

This explanation by Wilson et al. ignored another possible interpretation as pointed out by Nicholls and Petersen (1974), Malmström (1974), and Wikström et al. (1976). In the alternative explanation, the deduced spectral assignments for heme *a* and heme a_3 are retained and no heme–heme interactions involving ∈ are assumed. Instead, a heme–heme interaction that influences electron binding affinities (i.e., E_m's) is assumed.

Using isolated cytochrome *c* and cytochrome aa_3, Nicholls and Petersen (1974) determined the steady-state levels of ΔA at 551–540, 605–630, and 445–455 nm as functions of very low levels of $[O_2]$ (<0.1 μM). Assuming fixed and different contributions of hemes *a* and a_3 to

the Soret and α absorbances, the extents of reduction of the two centers as functions of $[O_2]$ were determined. The results were that at very low $[O_2]$, heme a_3 was much more reduced than cytochrome c, and heme a was much more oxidized. As $[O_2]$ was raised, there was a crossover such that heme a became more reduced than cytochrome c and heme a_3 became more oxidized. An independent kinetic method was used to obtain the steady-state level of a_3^{2+} as a function of $[O_2]$. If it is assumed that the rate-limiting step in the oxidation of cytochrome c is the transfer of electrons from ferrous cytochrome c to ferric cytochrome a_3, then dividing the rate of oxidation by $[c^{2+}]$ should yield a quantity that is proportional to $[a_3^{3+}]$, assuming that back reactions are negligible in the steady state. This alternative estimate of $[a_3^{3+}]$ produced a curve for percent of oxidation versus O_2 tension that resembled the one based on spectral data but gave lower levels in the central portion of the curve. The interpretation of these results was that heme–heme interaction exists where the redox state of heme a_3 controls the redox potential of heme a. At low levels of $[O_2]$, heme a_3 was largely reduced causing a reduction in midpoint potential of heme a, but at higher levels of $[O_2]$ when heme a_3 is largely oxidized, the heme a midpoint potential would be increased. If only two redox centers are considered, this kind of interaction must be symmetrical so that the reduction of heme a will make the reduction of heme a_3 more difficult. Such a situation should lead to a mixture of half reduced forms ($a^{2+}a_3^{3+}$ and/or $a^{3+}a_3^{2+}$) in the midrange of redox potentials. The overall picture is that the binding of the first electron to the fully oxidized form is relatively easy ($E_m > 280$ mV). This electron is viewed as being shared equally between heme a and heme a_3 in a form of rapid equilibration between the two partially reduced forms. The presence of the first electron renders the binding of the second more difficult so that the corresponding $E_m < 220$ mV. The sharing of the electron between hemes a and a_3 in the partially reduced state blurs the single identities of the two species. The two equal titration steps seen by Wilson et al. would then reflect this negative cooperative interaction rather than the titration of individual species of heme a and heme a_3. This view of the redox behavior of cytochrome c oxidase has become known as the "neoclassical model."

A more formal, mathematical presentation of this model was provided by Malmström (1974), who, in a general manner, considered the quantitative consequences of heme–heme interactions that can affect redox potentials and/or $\in$. He pointed out that, in principle, the results obtained thus far could be explained both in terms of redox interactions and spectral interactions. By altering the interaction parameters in the model, he could also account for the results of a titration performed in the presence of CO. Our presentation of the two center, two electron model in part 4 shows how it can, indeed, resolve the apparent dilemma created by results of Wilson et al. regarding the potentiometric behavior of cytochrome c oxidase.

The formulation of the negatively cooperative two site, two electron (neoclassical) model was a milestone in research on cytochrome oxidase. Not only did it offer an alternative explanation of the paradox between redox titration and the apparent amounts of cytochromes a and a_3, but it also illustrated a mechanism that may be an important aspect of the function of cytochrome oxidase. Whereas strictly optical interactions for this enzyme have no direct functional implications, redox interactions could be involved in facilitating electron transfer and (see below) coupling to proton pumping (Kamp et al., 1988).

In a completely different approach, Wikström et al. (1976) also challenged Wilson et al.'s interpretations, and they presented independent evidence in favor of the neoclassical model. The hypothesis of Wilson et al. that heme–heme interaction is expressed in terms of an enhancement of the $\in$ for heme a at 605 nm when heme a_3 is liganded was subjected to an experimental test. At the basis of this test is the assumption that the liganding of CO to heme a_3^{2+}, completely protects heme a_3^{2+} from oxidation by $K_3Fe(CN)_6$. By subjecting fully reduced and CO-liganded enzyme (in beef heart mitochondria) to $K_3Fe(CN)_6$ oxidation, they produced the mixed valence oxidase ($a^{3+}a_3^{2+} \cdot CO$). In another case, the fully reduced liganded species was produced ($a^{2+}a_3^{2+} \cdot CO$). These two preparations were placed in optical vessels in the dark and chilled to $-80°C$ in the presence of buffer and 30% ethylene glycol. The bottom portion of each cuvette was subjected to strong illumination to dissociate the ligand from heme a_3, and a difference spectrum of the dark (top) liganded form of the enzyme minus the bottom unliganded form of the enzyme was taken for each species. If, as according to Wilson et al., the absorbance of heme a^{2+} in the 605-nm region is greater when heme a_3 is liganded than when heme a_3 is free, then the magnitude of absorbance of heme a^{2+} in the top portion of the tube should be greater than the magnitude of heme a^{2+} absorbance in the bottom part, where heme a_3 is no longer liganded. This effect should lead to either a peak in the region of the α absorbance in the difference spectrum or at least a less extensive trough for the fully reduced species compared with the mixed valence species. It was found, however, that the trough for the difference spectrum in the case of the fully reduced enzyme was more pronounced than that seen with the mixed valence enzyme. This finding (Wikström et al., 1976) was interpreted as a direct proof of the invalidity of the Wilson et al. interpretation of optical interaction, hence as a support of the two site, two electron (neoclassical) model with heme–heme negative redox cooperativity. It should be noted, however, that this proof is not complete. It is perhaps not at all likely that CO has a *direct* effect on the absorption spectrum of heme a. If there was any effect on the spectrum, it would be *indirect* involving a confor-

mational change of cytochrome oxidase. The relaxation of such a conformational change could well be greatly retarded at 193 K. Independent evidence for just this kind of interaction was discussed above.

Looking back: a critical consideration of where we are

Preparations of cytochrome aa_3 at any voltage exhibit overlapping spectra consisting of the reduced and oxidized species of the two hemes, the mediators, and a varying amount of light scattering. Moreover, the existence of redox and other forms of cooperativity complicates the spectral overlaps in that chromophoric centers can undergo apparent changes of E_m leading to anomalous changes of absorbance with voltage and alterations in the shape of spectra. Therefore, information collected as a difference in absorbance across two wavelengths is ambiguous; all of the spectra present, including the light-scattering background, cut across these two wavelengths. If two of the spectra have absorbance peaks close to each other, then the overlap becomes more severe. There will not be a constant percentage of the contributions of each to the ΔA at all voltages unless the two centers have identical E_m's and the same n values. In addition to the uncertainties in the kinds of information contained in data expressed as two wavelength ΔAs, the method of analysis that led the early workers to conclude that only two $n = 1$ centers were present and that only two equal steps in the titration occurred is not capable of resolving the behavior of more complicated mixtures of chromophores. The problems associated with the use of these graphic procedures for analysis of E versus log (ox/red) representation of titration data have been discussed in detail elsewhere (Shrager and Hendler, 1986). In the experience of one of these authors (R. W. Hendler), data obtained from titrations of cytochrome aa_3, either in situ in mitochondria or in isolation, when analyzed by the traditional E versus log (ox/red) method using two point ΔA (605–630 nm) data do in fact lead to the conclusion that only two $n = 1$ centers are present in equal amounts and with the same E_m's reported by Wilson et al. However, more extensive analysis using all of the spectral information and more powerful analytical techniques have shown that the two equal $n = 1$ steps are not what is happening. The apparent single $n = 1$ titration at $\sim$230 mV can be resolved into two $n = 2$ titrations with E_m values near 200 and 260 mV (Hendler et al., 1986; Reddy et al., 1986). The graphic method of analysis cannot distinguish between a single $n = 1$ titration and two closely occurring $n = 2$ titrations.

The two equal $n = 1$ steps seen by Wilson et al. (1972), Wilson and Leigh (1974), Leigh et al. (1974), Tiesjema et al. (1973), Hendler et al. (1986), Reddy et al. (1986), and others are the consequence of analyzing two point ΔA data (605–630 nm) by the graphic E versus log (ox/red) resolution procedure. Because of the fundamental limitations in this method, the two steps do not necessarily represent separate titrations of two $n = 1$ heme centers, each accounting for $\sim$50% of the total absorbance. Therefore, there is no conflict in the results of the potentiometric titration of mammalian cytochrome aa_3 and the strong indications of earlier workers that heme a accounts for most of the ΔA at 605 nm. Using improved methods of data collection and analysis (discussed below), our resolved reduced minus oxidized spectra for cytochromes a and a_3 confirm the conclusions of the earlier workers on the disparity of the contributions of cytochrome a and a_3 to the 605-nm region (Hendler et al., 1986; Reddy et al., 1986) without, however, reversing the notion of redox cooperativity between the centers.

2. A FRESH LOOK AT AN OLD CONTROVERSY

Indeed, there are now better ways to analyze and resolve the results of potentiometric titrations of mixtures of cytochromes (Shrager and Hendler, 1982, 1986; Hendler et al., 1986). The titration of a single redox center causes a change in the ratio of two unique spectra (i.e., reduced and oxidized). The amplitude of the resulting difference spectrum will be a function of voltage. If two independent redox centers having different absorption spectra are present, the difference spectrum at any voltage range will be the sum of a factor times the difference spectrum of one redox center plus a different factor times the difference spectrum of the other center, each factor obeying the Nernst law. In other words, the difference spectrum will be a redox potential-dependent, linear, combination of the (constant) difference spectra of the two centers. If the two redox centers have cooperative interactions such that reduction of the one affects the apparent midpoint potential of the other, the spectrum at any voltage will still be a linear combination of the same two difference spectra, although the linear combination will be different; the factors not now obeying the simple Nernst law.

The resolution of a series of spectra, obtained from a multiredox center sample, into individual spectral components can be viewed as a problem in linear algebra. If spectra comprising 200 wavelengths are acquired during a potentiometric titration at 100 voltages, then the raw data can be expressed as a matrix, **A**, with 200 rows and 100 columns. The information contained in each column is strictly spectral. Each row of the matrix shows the titration behavior of the mixture at a particular wavelength. If there is only a single redox center, then the changes between the subsequent columns arise from the further reduction (or oxidation) of the component. If there are several redox centers, the subsequent columns accumulate the further reductive (or oxidative) changes of all of these components. However, the contributions of the separate spectra differ according to their E_m's and n values. Typically, at ambient voltages close to the E_m of a center, **X**, the spectral change due to **X** will contribute

more than the spectral change due to Y with an E_m much higher or lower than that of X. The challenge is to find out at how many positions along the columns, a maximum contribution of a center, occurs (i.e., how many independent redox centers there are). This challenge can be met most effectively and objectively by deconvoluting the input matrix according to principles of linear algebra into three factor matrices by the procedure of singular value decomposition (SVD) (Shrager and Hendler, 1982). In one matrix (U), only spectral information is contained. Each column is an "eigenspectrum." Together, the eigenspectra can account for the entire spectral variation during the redox titration. These eigenspectra exhibit special mathematical properties; they are orthonormal and are so-called eigenvectors of the matrix, $\mathbf{AA}^T$. They are not the spectra of individual cytochromes. When absolute spectra are analyzed, the number of these eigenspectra that are significantly different from background noise (i.e., the rank) is equal to the number of linearly independent spectral components plus one for a reference state. That is, if cytochromes *a* and a_3 have different spectra and spectral cooperativity is absent, then three eigenvectors will be found for a redox titration passing through both midpoint potentials independently of whether there is redox cooperativity. If there is spectral cooperativity, four eigenvectors may be found depending on the nature of the interaction. In reality, it is perhaps naive to think that either redox or spectral cooperativity can occur independently. The conformational and electronic changes that are implied are likely to affect both the E_m's and spectra of redox centers. If the input matrix, A, contains difference spectra obtained by the subtraction of a reference spectrum from all of the absolute spectra, then the number of eigenvectors will be reduced by one (i.e., the reference eigenvector is eliminated).

Each spectral eigenvector varies its amplitude as a function of voltage in a unique manner. A second factor matrix (V) obtained through SVD contains precisely this information. The columns of V are eigenvectors of the matrix $\mathbf{A}^T\mathbf{A}$. The first column of the V matrix contains the titration information for the first eigenspectrum of the U matrix.

The third matrix (S) is a diagonal matrix. Its elements are the relative weights by which the eigenspectra contribute to the observed spectral titration. The columns of U, V, and S correspond to each other and are ordered with respect to decreasing absolute magnitude of the relative weights (equal to the square roots of the eigenvalues). Usually, four to six columns of the factor matrices contain virtually all of the information describing the titration behavior of the sample.

A final step in the analysis attempts to produce the difference spectra of the true redox centers from the eigenspectra. Here, the information is used that redox centers mostly titrate in a well-defined manner with redox potential. Specifically, this involves the fitting of the columns of V to expressions containing combinations of Nernstian functions, which then dictates how the columns of U must be combined to produce the difference spectra emanating from individual redox centers in the mixture. It should be noted, however, that it is possible for strong redox interactions to produce non-Nernstian behavior. This situation would lead to poor fittings with large nonrandom residuals. Our data showed no indications of non-Nernstian behavior. The complete analysis yields the difference spectra, amounts, E_m's, and *n* values of the individual cytochrome components.

SVD analysis of a large series of redox titrations of pure cytochrome aa_3 from beef heart and *Paracoccus denitrificans* and in intact beef heart mitochondria has led to the finding of three distinct Nernstian redox transitions. Since, however, the number of eigenvectors found was higher than three, cooperative spectral interactions are implicated.

Although the SVD method of data analysis is much more capable of resolving the contributions of individually titrating spectral components than the previously used graphic procedures based on two point ΔA data (Shrager and Hendler, 1986), it is still important to verify the results by independent means. For this purpose, we have used analyses based on the second derivatives of absorbance versus wavelength at wavelengths of interest. The magnitudes of the second derivatives are computed from the absorbance at a central wavelength position and that at 10 other wavelength positions spaced equally on both sides of the peak. The rational is that the magnitude of the second derivative is proportional to the size of the peak, but absorbances from other spectra cutting across these 11 wavelength positions contribute much less to the second derivative than does the spectrum of interest. Therefore, the second derivatives have much less ambiguous information than do the two point ΔAs. If SVD indicates a spectrum with a particular Soret peak, α peak, E_m, and *n* value, then the two second derivatives, for the Soret and α peaks, should yield the same E_m and *n* value as each other and as the SVD analysis. The analyses of the second derivative data have been based on nonlinear least-squares analyses of sums of Nernst expressions using statistical "best fit" criteria (Hendler et al., 1986).

Resolution of the potentiometric titration data for cytochrome aa_3 based on combined SVD and second derivative analyses

The three Nernstian transitions discovered by the combined approach showed unique optical difference spectra and titration properties (Hendler et al., 1986; Reddy et al., 1986; Pardhasaradhi et al., 1991). There was a component with E_m near 190 mV, $n = 2$, Soret maximum near 428 nm, and α maximum near 602 nm. A second component was seen with an E_m near 260 mV, $n = 2$, Soret maximum near 446 nm, and α maximum

near 605 nm. The third component had an E_m near 340 mV, $n = 1$, Soret maximum near 448 nm, and α maximum near 607 nm. The second and third components showed distinct troughs near 428 nm.

SVD analysis of titrations performed in the presence of CO produced the same difference spectra and similar Nernstian properties for the 260- and 340-mV components. However, the unique spectrum for the component titrating at 190 mV was absent. In its place was the characteristic spectrum for CO-liganded reduced heme a_3 with a Soret maximum near 433 and α maximum near 593 nm. On this basis, the spectrum described above for the 190-mV component in the absence of CO was identified with cytochrome a_3. The other $n = 2$ and $n = 1$ components are ascribed to the titration of two different forms of cytochrome *a*. This requires that the heme *a* be electronically (because of the difference in n) and optically coupled with some other center (Cu_A?) in one case but not the other. Difference spectra showed the characteristic Soret and α peaks for cytochrome *a*, as well as the disappearance of the Soret peak at ~428 nm identified, as described above, with cytochrome a_3. The presence of three Nernstian transitions, in the titration of mammalian cytochrome aa_3, with E_m values near 200, 260, and 340 mV, has since been confirmed by Steffens and Buse (1988) and by Nicholls and Wrigglesworth (1989). No experimental identification of the three transitions in terms of cytochrome *a* or a_3 was provided, however.

Subsequent studies have shown that the titration seen at ~190 mV for cytochrome a_3 also consists of two different forms of this cytochrome (Sidhu and Hendler, 1990). One form is favored by the presence of a lipoprotein matrix, provided either by the mitochondrial membrane or in the form of a liposomal membrane or a supplement of added lipoprotein. The formation of the membrane-stabilized form is facilitated by holding the enzyme at a voltage of >400 mV in the presence of ~1 mM $K_3Fe(CN)_6$ for ≥30 min before the titration. Under these conditions the predominant form of reduced cytochrome a_3 shows a Soret peak near 428 nm, a prominent α peak near 602 nm, and an E_m near 175 mV. In the absence of the lipoprotein, pre-exposure to the high voltage, and titration in the presence of ~1 mM $K_3Fe(CN)_6$, the reduced cytochrome *a* shows the typical Soret peak near 446 nm, a much smaller α peak, and an E_m near 200 mV. Both species of reduced cytochrome a_3 form complexes with CO, resulting in a shift of the Soret absorbance to near 433 nm and the α absorbance to near 593 nm. The CO complex made from the lipoprotein-associated form of cytochrome a_3 has an E_m near 230 mV, and the CO complex made from the free form of cytochrome a_3 has an E_m near 330 mV. The shift in Soret location from 446 to ~428 nm is indicative of a high to low spin transition. A number of literature reports describe a low spin form of cytochrome a_3 that arises during turnover or energization of the enzyme. Nicholls and Hildebrandt (1978) described a low spin form with a Soret peak at 433 nm formed during turnover of the purified enzyme, mitochondria, or submitochondrial particles. More recently, Nicholls and Wrigglesworth (1989) concluded that the reduction of Cu_B was the trigger that started the transformation of cytochrome a_3 to the low spin form. Wrigglesworth et al. (1988) have correlated the apparent spin state transition during turnover of the initially resting enzyme with the generation of a fast-reacting form of cytochrome a_3 with respect to either reduction or binding of CN^-. A further correlation was made with the disappearance of a g = 12 EPR signal used by Baker et al. (1987) as an indicator of the slow reactive species of cytochrome a_3. Spiro and coworkers (Ray et al., 1990) have used resonance Raman spectroscopy to reveal a low spin form of reduced cytochrome a_3 induced by the addition of ATP to submitochondrial particles. It also may be recalled that >30 years ago, Okunuki et al. (1957) described a shift in the location of the Soret peak from ~420 to ~428 nm and of the α peak from ~605 nm to near 602 nm, accompanying a transformation of the enzyme from a sluggish to a more reactive form. For a more complete discussion and contemporary assessment of the "pulsed" form of cytochrome oxidase, see Brunori et al. (1988).

A unique manifestation of redox cooperativity was indicated in the titrations of cytochrome aa_3, when complete optical spectra were used (Hendler et al., 1986). Both by the SVD procedure and second derivative analyses centered at 429 nm, the reduction of cytochrome *a* as the voltage was lowered from 450 to 200 mV was accompanied by the apparent, anomalous oxidation of cytochrome a_3, as indicated by the loss of the spectrum with a peak near 429 nm, identified above as emanating from cytochrome a_3. Titration below 200 mV caused the re-reduction of cytochrome a_3 as manifested by the reappearance of the peak near 429 nm. The conclusion that a reverse titration of cytochrome a_3 was actually occurring was based on a number of observations and reasons discussed in detail in Hendler et al. (1990). Some of these are listed below and further discussed in part 4.

(*a*) Because cytochrome a_3 is the direct donor of electrons to O_2, it is expected to have an E_m between that of cytochrome *a* and O_2. Cytochrome a_3 has at least one E_m near 200 mV (Sidhu and Hendler, 1989; Harmon, P., R. W. Hendler, and I. Levin, manuscript in preparation). A second and significantly higher E_m species is, therefore, expected.

(*b*) Direct evidence for a higher E_m species of cytochrome a_3 was obtained in two ways. When fully oxidized cytochrome aa_3 is placed in a medium held at any voltage between 450 and 750 mV, the feature with a peak at 429 nm appears. This feature again disappears as the voltage is raised above 750 mV.

(*c*) The behavior of the 429-nm feature as the voltage is raised from ~100 to ~780 mV is what would be expected for a system that displays two E_m's for the same redox center. The feature diminishes as the voltage

passes across the lower E_m, rises as it approaches the higher E_m, and diminishes again as the voltage exceeds the higher E_m.

(*d*) The rise in 429-nm feature that occurs in the voltage range 230–400 mV cannot be attributed solely to the increase in amount of oxidized species of cytochrome *a* as the voltage is increased.

3. STRONG COOPERATIVITY IN CYTOCHROME aa_3

To explain the apparent oxidation of cytochrome a_3 as the voltage was lowered and the subsequent re-reduction of the cytochrome below 200 mV, we considered and explored stronger forms of redox cooperativity than those present in the "neoclassical" model. For cytochrome a_3 to be in a reduced state at a voltage of ~450 mV, it must have an E_m higher than this voltage. However, the titration of cytochrome a_3 in two different forms was demonstrated at ~190 mV (Sidhu and Hendler, 1989). The behavior observed could be explained if the E_m of cytochrome a_3 was controlled by the redox state of another center, which we shall call *X*. When *X* is oxidized, cytochrome a_3 has an $E_m \gg 450$ mV, but when *X* is reduced, the E_m of the cytochrome is below 200 mV. At 450 mV, *X* is oxidized and cytochrome a_3 will be reduced. In a reductive titration, as *X* becomes reduced, the E_m of cytochrome a_3 drops below 200 mV. If the voltage of the medium is >200 mV, cytochrome a_3 will become oxidized. Below 200 mV, the cytochrome will be reduced as expected according to its low E_m. The neoclassical model also allowed for redox interactions. However, these were not strong enough for the reduction of one redox center to cause the oxidation of another. Indeed, for thermodynamic reasons (discussed in part 4), a two-center, two-electron system cannot exhibit such a phenomenon. Key to the "modern models" proposed here is the strong cooperativity resulting from the interactions of at least three electrons, leading to the inverse redox behavior of a redox center (cytochrome a_3). In part four, we will show that a fuller thermodynamic treatment, which allows for strong cooperative interactions, can accommodate the experimental data.

Additional support for these "modern models" came from the observations that if (oxidized) resting cytochrome aa_3 is placed into a medium with the voltage preset from 450 to 750 mV, the Soret peak shifts from its resting position near 420 nm to a new position near 428 nm (Hendler and Sidhu, 1988). In the voltage range 750–790 mV, the peak shifts back toward 420 nm. The high voltage titrations were performed in the presence of metallo cyanide complexes of Fe, W, and Mo. It was shown that the shift in Soret position from 420 nm to near 428 nm that occurs at high voltage could not be explained by the release of CN^- from the metallo cyanide mediators (Hendler et al., 1990). Additional observations were cited in support of the presence of a high voltage form of cytochrome a_3. Wikström (1987, 1988), using a different approach, has also concluded that a high voltage transition of cytochrome a_3 exists. Interestingly, in his case the cooperative interaction was proposed to be with the membrane potential.

All of the observations described above for cytochrome aa_3, including three Nernstian transitions, two forms of low potential cytochrome a_3, a high potential form of cytochrome a_3, and the interactive redox behavior described for the mammalian enzyme, were seen also in cytochrome aa_3 isolated from *P. denitrificans* (Pardhasaradhi et al., 1991). The identification of a low voltage form of cytochrome a_3 titrating near 200 mV was independently confirmed using resonance Raman spectroscopy (Harmon, R., R. W. Hendler, and I. Levin, manuscript in preparation). This same study has uncovered yet another form of low potential cytochrome a_3, with an E_m near 259 mV.

The newer findings revealed by the SVD and second derivative analytical techniques and the inability of the neoclassical cooperative model to explain these findings were the stimulus to the further theoretical development of redox cooperativity described in this article. Recently, Nicholls and Wrigglesworth (1989) also pointed out the inadequacy of the neoclassical model to explain a biphasic shift in the E_m of one redox center when another center is titrated and the subsequent phenomena of the oxidation of one cytochrome as another is being reduced, as reported from our laboratory and earlier by Kojima and Palmer (1983). A newer model proposed by Nicholls and Wrigglesworth (1989) involves three electrons and includes Cu_B in addition to the two hemes. A constraint built into this new model is that Cu_B must be reduced before cytochrome a_3. This model cannot explain the redox behavior of cytochrome aa_3 described in this article. One other observation, totally incompatible with the neoclassical model, is that the potentiometric behavior of cytochrome a_3 is distinctly different from that of cytochrome *a*. This has been established with two different techniques that unambiguously distinguish between cytochrome a_3 and cytochrome *a*. One is the ability to react with CO (Hendler et al., 1986), and the other is potentiometric titrations monitored by resonance Raman spectroscopy (Harmon, P., R. W. Hendler, and I. Levin, manuscript in preparation).

4. MODELING OF DIFFERENT KINDS OF REDOX COOPERATIVITY INVOLVING CYTOCHROME aa_3

The experimental data used for testing the models in this article were obtained in an electrical reductive titration of pure cytochrome aa_3, under conditions that favor the formation of a low spin form of cytochrome a_3 (Hendler et al., 1986). The ordinate values for figures showing the

results of fittings to the models represent the negative second derivatives of the peak absorbance features centered at 428 nm for cytochrome a_3 and at 604 nm for cytochrome a. The range of magnitudes of the values for cytochrome a was about one-fourth that for cytochrome a_3. For illustrative purposes, the cytochrome a values were normalized to the range for cytochrome a_3. In the fitting procedure, the values for all E_m's were simultaneously fit to both sets of data (i.e., for cytochrome a and cytochrome a_3). All fittings to the various models, as well as all of the graphics shown in this article, were performed using the software package MLAB (Civilized Software, Inc., Bethesda, MD) run on a personal computer with an Intel 80386 processor and an Intel 80837 math coprocessor.

Although the electron does not exist as a free entity in solution, it does have both a chemical and an electrochemical potential, and its binding to an oxidized center is analogous to other ligand binding reactions both thermodynamically and mathematically (Walz, 1979; Hill, 1985). This view is useful in considering cooperativity between and among redox centers wherein the binding of an electron at one center may change the binding affinity (i.e., E_m) at another center. Although the significance of the E_m value in a Nernstian expression is readily appreciated as the voltage where the concentrations of oxidized and reduced species are equal, the significance of the n value is a bit more subtle. The Nernst equation shows that for each incremental change of voltage of $60/n$ mV, the ratio of [R]/[O] changes by a factor of 10. The amount of energy needed to change the ratio of product to reactant, by a factor of 10, for a chemical reaction at 25° is ~5.7 kJ. The amount of energy released by an electron passing through a voltage increment is given by the Faraday constant as 96.4 J/mV. If only one electron is involved (i.e., n) = 1), then a voltage change of 59.2 mV is required for 5.7 kJ. For an $n = 2$ redox reaction, two electrons moving across a 29.6-mV increment is sufficient. When an $n = 2$ value is assigned to an apparent $n = 1$ center (i.e., heme a), it is implied that this center is coupled to a second, unspecified center (e.g., Cu_A). Strong cooperative interactions for electron binding between two $n = 1$ centers can produce $n = 2$ behavior, such that the states (R, O), and O, R) are extremely nonprobable and states (O, O) and (R, R) are highly probable. Using Eqs. 1–4, one may write the relative concentrations of the states OO, RO, OR, and RR, as 1, $K_{RO} \cdot \phi$, $K_{OR} \cdot \phi$, and $K_{RR} \cdot \phi^2$, respectively. Whenever K_{RR} greatly exceeds both K_{OR} and K_{RO}, such strong cooperativity obtains. The 30 mV per decade response of this system is seen in the term ϕ^2, which is equal to $10^{-E/60})^2 = 10^{-E/30}$ (cf. Eq. 11).

Two-site models

Two electron model

The neoclassical anticooperative model that involves two sites and two electrons is the simplest cooperative model that can be constructed and is shown in Fig. 1. The redox state of each heme is indicated by an O (oxidized) or R (reduced), with the left side representing heme a_3 and the right side heme a. The letter in parentheses shown for each E_m term indicates the redox state of the center not undergoing a redox change. An essential constraint for this and for the more complicated interactive models that we will construct below is invoked by the principle of microscopic reversibility that requires that the sum of the products of the n values and the E_m values for all sequential reactions connecting any two states be the same, regardless of the route followed (e.g., Westerhoff and van Dam, 1987). This is because the ΔG^0 between the two states is unaffected by the route and because $\Delta G^0 = -nF\Delta E^0$. The only, but interesting, allowable deviation from microscopic reversibility occurs when one of the paths connecting two states is coupled to another nonequilibrium reaction, such as proton pumping (Westerhoff and van Dam, 1987). However, in the experiments analyzed here, proton gradients are absent.

In the specific elaboration of the two-site, two electron model, which has been called the neoclassical model, the first electron is bound with equal affinity by either heme a or heme a_3 (i.e., $E_{ma3}(O) = E_{ma}(O)$). The presence of this electron inhibits the binding of the second electron to the other heme so that $E_{ma3}(R) < E_{ma3}(O)$ and $E_{ma}(R) < E_{ma}(O)$. Because of the constraint on the sums of E_m's, $E_{ma3}(R) = E_{ma}(R)$. This model was used to explain observations based on the ΔA (605–630 nm) and analyzed by the graphic E versus log ox/red procedure (as discussed in part 1). In this context, $E_{ma3}(O) = E_{ma}(O) \approx 360$ mV and $E_{ma}(R) = E_{ma}(R) \approx$

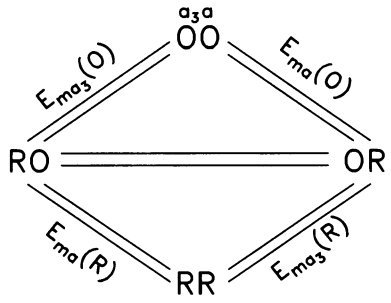

$$E_{ma3}(O) + E_{ma}(R) = E_{ma}(O) + E_{ma3}(R)$$

$$E_{ma3}(O) = E_{ma}(O) > E_{ma}(R) = E_{ma3}(R)$$

FIGURE 1 The two-site, two-electron (i.e., neoclassical) model. The site on the left represents heme a_3 and the site on the right, heme a. The oxidation state of the site is indicated by O (oxidized) or R (reduced). The term in parentheses for each of the E_m's shows whether the site not undergoing a redox change is in the oxidized or reduced state. The condition for negative cooperativity is indicated by the bottom equation in the figure.

240 mV. The negative redox cooperativity between the two redox centers is reflected in that 240 < 360 mV. The method used in our approach is standard and based on the partition function method as reviewed by Hill (1985) and Di Cera (1990). Here, we shall keep the partition functions implicit (cf. Hill, 1985).

For our analysis of this simple model, the Nernst equation for $n = 1$ is restated as

$$R = O \cdot K \cdot \phi, \tag{1}$$

where R = [reduced species], O = [oxidized species], $K = 10\,\hat{}\,(E_m/60)$, $\phi = 10\,\hat{}\,(-E/60)$, and E is the ambient redox potential in mV and, E_m, the midpoint potential at ambient conditions (including pH). The number 60 derives from $(RT/F) \cdot \ln(10)$ in mV and should be replaced by the latter at other than 300 K temperature.

Using these terms, the concentrations of each of the four states can be expressed as functions of voltage. For the parameter values cited above, this yields:

$$RO = OO \cdot K_{RO} \cdot \phi = OO \cdot 10\,\hat{}\,(360/60) \cdot \phi, \tag{2}$$

$$OR = OO \cdot K_{OR} \cdot \phi = OO \cdot 10\,\hat{}\,(360/60) \cdot \phi, \tag{3}$$

$$RR = OO \cdot K_{RR} \cdot \phi^2 = OO \cdot 10\,\hat{}\,((360 + 240)/60) \cdot \phi^2, \tag{4}$$

$$\begin{aligned} T &= OO + RO + OR + RR \\ &= OO \cdot (1 + 2 \cdot 10\,\hat{}\,(360/60) \cdot \phi \\ &\quad + 10\,\hat{}\,(600/60) \cdot \phi^2), \end{aligned} \tag{5}$$

$$\therefore OO = T/(1 + 2 \cdot 10^6 \cdot \phi + 10^{10} \cdot \phi^2). \tag{6}$$

The total amount of reduced heme a is represented by $OR + RR$ and that of heme a_3 by $RO + RR$. Because $OR = RO$, the fraction of reduced heme a as a function of voltage equals the fraction of reduced heme a_3 as a function of voltage. This is true even if heme a contributes 80% to the absorbance at A_{605} and heme a_3, only 20%:

$$\Delta A_{605} = 0.8 \cdot [OR] + 0.2 \cdot [RO] + [RR]. \tag{7}$$

Because $[OR] = [RO]$

$$\Delta A_{605} = RO + RR = OR + RR. \tag{8}$$

Therefore, the equal two-step titration shown in Fig. 2 would be expected from an experiment monitoring ΔA_{605}, even if 80% of the ΔA is due to just one heme. As pointed out by Nicholls and Pedersen and Malmström (1974), this model offers an explanation for the paradox posed by the findings of Wilson and collaborators (part one). It does not account, however, for newer findings that show an oxidation of cytochrome a_3 as the voltage is lowered from ~450 to ~200 mV and the re-reduction of cytochrome a_3 below 200 mV. It also does not account for the $n = 2$ and $n = 1$ titrations of cytochrome a seen at 260 and 340 mV. Finally, it ignores the possibilities for redox interactions involving the other centers in the cytochrome oxidase complex.

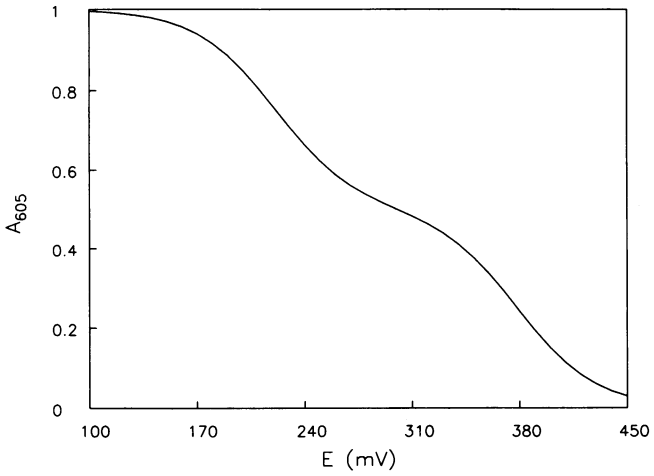

FIGURE 2 Theoretical titration of two heme centers that account unequally to the total absorbance, according to the neoclassical model shown in Fig. 1. In this representation, the E_m's and percentage contribution to the total absorbance were 360 mV and 80% for heme a and 240 mV and 20% for heme a_3.

The inability of a two-electron, two-center model to account for a turnaround in the titration of a given redox center (i.e., heme a_3) can be rigorously shown.

Let $pra_3 = (RO + RR)/(OO + RO + OR + RR)$

$$pra_3 = \frac{K_{RO} \cdot \phi + K_{RR} \cdot \phi^2}{1 + K_{OR} \cdot \phi + K_{RO}\phi + K_{RR} \cdot \phi^2}. \tag{9}$$

The question is whether $dpra_3/d\phi$ can equal zero. The solution to the quadratic equation that results is that for $dpra_3/d\phi = 0$, $K_{OR} \cdot K_{RO}/K_{RR}$ must equal 0. Because all of the Ks are positive, this condition cannot be met, and therefore no maximum nor minimum in a plot of pra_3 versus E is to be expected.

Three electron model

The addition of a third electron to the two-center model, however, does allow for a turnaround in the plot of pra_3 versus E (e.g., if the reduction of cytochrome a required two electrons, whereas that of cytochrome a_3 required only one). Using this model, we tried to simulate the redox behavior seen for cytochrome a and cytochrome a_3 experimentally. For this endeavor, as well as for similar exercises using more complicated models, we have adopted an approach that fits all E_m values in a thermodynamically consistent manner. This means that the sum of the products of $E_m \times n$(umber) of electrons transferred, for all paths connecting two redox states must be the same. Rather than fitting each E_m linking two sequential redox states individually, we attribute a redox potential (standard free energy) (Westerhoff and van Dam, 1987) to every state and fit these standard redox potentials to the experimental data. For example, if the fully oxidized state, OO, is taken as the reference,

then,

$$RO = OO \cdot 10\hat{}((E_{mRO} - E)/60) \quad (1 \text{ electron}), \tag{10}$$

$$OR = OO \cdot 10\hat{}((E_{mOR} - E)/30) \quad (2 \text{ electrons}), \tag{11}$$

$$RR = OO \cdot 10\hat{}((E_{mRR} - E)/20)) \quad (3 \text{ electrons}), \tag{12}$$

$$OO = T/(1 + 10\hat{}((E_{mRO} - E)/60) + 10\hat{}((E_{mOR} - E)/30) + 10\hat{}((E_{mRR} - E)/20)). \tag{13}$$

The standard redox potential (E_m) terms in the exponents relate each state to the OO state, and the denominator in the exponent is $60/n$. In this way, the E_m, is equal to the sum of the products of $\Delta E_m \times n$ for all of the intermediate redox steps divided by the sum of the n values, where ΔE_m refers to the midpoint potential of a redox transition. The amounts of reduced cytochrome a and a_3 are represented as

$$fra = OR + RR, \tag{14}$$

$$fra3 = RO + RR. \tag{15}$$

We shall here use the experimental data for cytochrome a, obtained as a plot of the magnitude of the second derivative at 604 nm versus E. The reason for using second derivative data for this purpose rather than SVD data is as follows. The SVD method produces titration curves for each of the eigenvectors of the spectral components. It does not yield titration curves for the individual redox species present. Difference spectra for each of the species are deduced after modeling the titration eigenvectors and then mixing the spectral eigenvectors as directed from the results of the fitting procedures. We have found that the E_m's, derived by SVD, are the same as found by using second derivatives at the unique wavelengths, characteristic of either cytochrome a_3 or a. The second derivative data for cytochrome a contain a small contribution from cytochrome a_3 because of the α absorbance of the latter at 602 nm. In the equation used for fitting, this is accounted for by including a fittable parameter (p) for a percentage of the titration of cytochrome a_3. Rather than assuming that the reference or baseline value for the second derivative is zero, the baseline is also fitted as a parameter (da) that does not vary with ambient redox potential, E. The modified expression used for fitting cytochrome a is then

$$frapa3 = fra + p \cdot fra3 + da. \tag{16}$$

The experimental data for cytochrome a_3 were obtained as a plot of the magnitude of the second derivative at 428 nm versus E. The fitting equation for cytochrome a_3 was also modified. It is always observed that more of the absorbance is lost in the titration range from 450 mV down to ~200 mV than is regained in the further titration down to ~100 mV. This could be due to cooperativity affecting the extinction of reduced cytochrome a_3 as influenced by the redox state of another center. This is allowed for by including a fittable extinction term (ex) to modify the contribution from the form of cytochrome a_3 represented as RO. An essential redox mediator used in all of the titrations is ferricyanide. The oxidized form of this compound has a prominent absorbance feature at 428 nm and an E_m of ~430 mV. It is therefore necessary to include a term for the titration of ferricyanide. Finally, a baseline term ($da3$) is also included. The fitting equation used for cytochrome a_3 is then

$$fra3exf = ex \cdot RO + RR + FCN/(1 + 10\hat{}((430 - E)/60)) + da3. \tag{17}$$

The results of fitting Eqs. 16 and 17 to experimental data are shown in Fig. 3. The fitted E_m's were 590, 418, and 348 mV for E_{mRO}, E_{mOR}, and E_{mRR}, respectively. This means that the E_m's for the individual steps $OO \rightleftharpoons RO$, $OO \rightleftharpoons OR$, $RO \rightleftharpoons RR$, $OR \rightleftharpoons RR$, and $RO \rightleftharpoons OR$ were 590, 418 ($n = 2$), 227 ($n = 2$), 208, and 246 mV, respectively. The fit is not close, and the model itself is unrealistic, but the cooperative interaction that can account for an oxidation of cytochrome a_3 as the voltage is lowered and cytochrome a is reduced, the heart of our "modern" models, is demonstrated.

A rigorous thermodynamic analysis of cooperative ligand binding interactions based on appropriate partition functions for electron binding recently has been presented by Di Cera (1990). In this treatment, Di Cera also has shown that at least three interacting ligand-binding

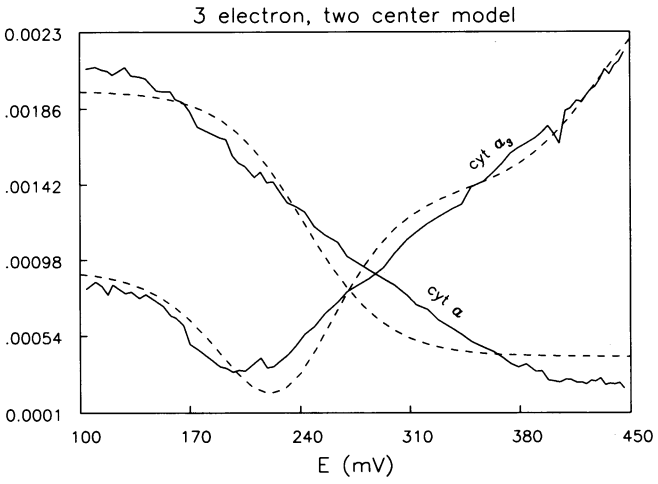

FIGURE 3 Fit of experimental titration data for cytochromes a and a_3, using a three-electron, two-site model. The titration data are expressed as the magnitudes of the second derivatives of absorbance versus wavelength at the peak wavelengths of 428 nm for cytochrome a_3 and at 604 nm for cytochrome a. The magnitudes and extent of the changes for cytochrome a_3 are about four times that involving cytochrome a. To have equal weights, however, in the simultaneous fitting of all of the E_m's to both sets of titration data, the cytochrome a data have been normalized to that of cytochrome a_3. This has been done for the fitting of all of the models described in this article. The computer fitting determined the E_m's that provided a best fit, using Eqs. 10–17. The dashed lines show the resultant fits for the cytochrome a_3 titration using Eq. 17 for "*fra3exf*" and for cytochrome a using Eq. 16 for "*frapa3*."

events must occur before local violations of the second law of thermodynamics are seen. Below, we explore increasingly more complicated models that take into account the other redox centers and possible effects of changes in conformational states or dimerization of the cytochrome oxidase.

Three-site models

In Fig. 4, a general three-site model is shown that involves five electrons and is consistent with our finding of three transitions having n values of 2, 2, and 1 (Hendler et al., 1986). The left-hand position designates a two-electron site that represents the heme a_3-Cu_B couple. The middle site is for heme a, which, depending on conditions specified below, can operate as a simple $n = 1$ site or as a coupled (i.e., to Cu_A) $n = 2$ site. The right-hand position represents another redox site (e.g., free radical and/or Cu). In dealing with this and still more complex models to be presented below, we have adopted a notation that has proven to be quite helpful. When more than a single reduced center is present in a particular couple such as with *OOR* and *ORR*, parentheses are used to designate the center that is undergoing oxidation or reduction. Thus, for the *OOR*/*ORR* couple, $E_{mO(R)R}$ is used.

The model shown in Fig. 4 is structurally simpler than other models presented afterward in that it has fewer states (i.e., 8). However, it is more complex in the sense that it entails a new kind of cooperativity other than that which affects E_m values and spectral properties. The ability of redox states of certain centers to influence the "n-ness" of other centers was introduced to account for the findings of $n = 1$ and $n = 2$ forms of cytochrome a

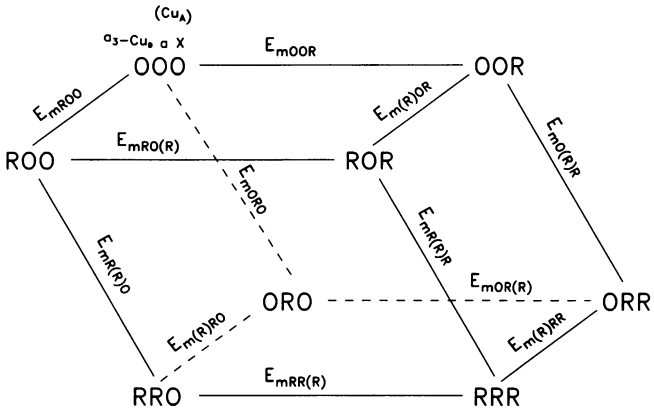

FIGURE 4 A general three-site model. The site on the left represents a coupled cytochrome a_3, Cu_B center. The middle site represents cytochrome a, and the site on the right represents an additional redox site, which could be the "extra" Cu recently found in several laboratories. For the single three-site model, five electrons are involved. Cu_A is not treated as a separate independent site. Its titration is expressed by coupling either with site X or heme a, raising the appropriate n value from 1 to 2. The term in parentheses in the subscript for the E_m's represents the site undergoing a redox change.

(Hendler et al., 1986). In the figure, all paths involve two electrons except for the transitions with $E_{mO(R)R}$, $E_{mOR(R)R}$, $E_{mR(R)R}$, and $E_{mRR(R)}$, which involve only a single electron. This leads to five electrons involved in the complete reduction of *OOO* to *RRR*, regardless of the route followed. There are at least two different ways one can visualize this kind of behavior. The spectral signature for the middle center is that of heme a. If in certain configurations Cu_A is close enough to heme a to allow coupling of the centers, then an $n = 2$ character would be seen for heme a, whereas center X would be $n = 1$. During the past 8 years, new evidence has pointed to a third Cu site in cytochrome aa_3 (Einarsdóttir and Caughey, 1984, 1985*a*, *b*; Bombelka et al., 1986; Steffens et al. 1987). This center is called Cu_X. For this model, consider center X to be Cu_X and allow for the possibility that in another configuration Cu_A could be electronically coupled to Cu_X so that heme a would be $n = 1$ and X, $n = 2$. The ability of heme and Cu centers to couple is well illustrated in the binuclear a_3-CuB center. The possibility of a coupled Cu_A-Cu_X binuclear center has been suggested by recent work of Kroneck et al. (1988, 1990). Another representation of the ability of cooperative interactions to affect the "n-ness" of heme a has the n values of both the a_3-Cu_B and X centers fixed at two. When X is oxidized, the heme a and Cu_A centers are coupled with $n = 2$. When X is reduced, the heme a and Cu_A centers are independent, and the E_m of Cu_A is so depressed that it cannot be reduced in the voltage range of interest. Other considerations could apply that would also account for the ability of redox states to affect "n-ness" of other centers. At this point, it is only important to describe this new kind of cooperativity and not to advance a particular model.

In cases where it is important to specify whether a particular center is operating as $n = 1$ or $n = 2$, the lower case character (o or r) will be used for one electron transitions and upper case (O or R) for two electron transitions. Cooperative interactions may be such that for any number of electrons in the enzyme, only some states are sufficiently low in standard free energy to occur at significant concentrations. It may even be such that at any ambient redox potential, a particular redox state, for example, *OOr*, occurring at a concentration of $OOO \cdot K_{OOr} \cdot \phi$ is insignificant compared with *OOR*, which occurs at $OOO \cdot K_{OOR} \cdot \phi^2$. Consequently, for a given enzyme, only states *OOO*, *ROO*, *OOR*, *OrR*, *RRO*, and *RRr* may occur, *RRR* only being attainable at extremely low ambient redox potentials. For transitions of the middle center, this implies that $R(R)O$ is $n = 2$, whereas $O(r)R$ is $n = 1$ (i.e., the redox states of a_3 and X determine whether a is a one- or two-electron center).

The specific details of this model were introduced with the aim of seeing whether a single three-site model could account for all of the experimental observations. The initial values assigned to E_m and n in this model were guided by experimental results. For example,

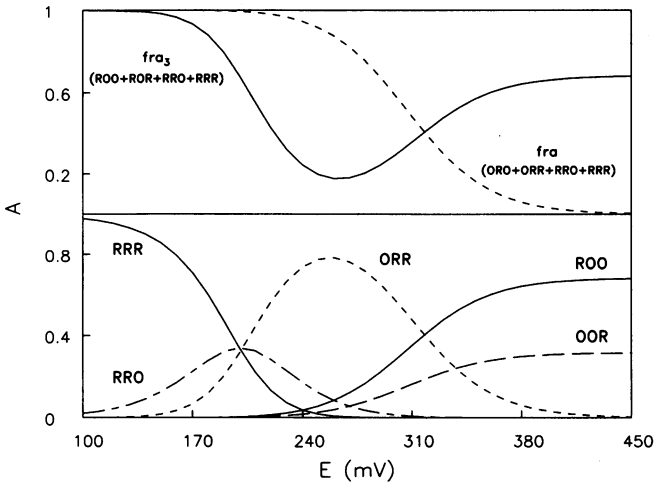

FIGURE 5 (*Top*) Theoretical titrations for cytochrome *a* (*dashed line*) and cytochrome a_3 (*solid line*) in the cooperative five-electron, three-site model illustrated in Fig. 4. The equations used in the simulation were numbers 27 (*fra*) for cytochrome *a* and 28 (*fra*3) for cytochrome a_3. (*Bottom*) Theoretical titrations for each of the individual partially and fully reduced states shown in the five-electron, three-site model in Fig. 4. The curves for states *ORO* and *ROR* are in the baseline. The equations used were numbers 19–26.

$$E_{\mathrm{mROO}} = 600, \quad n = 2,$$
$$E_{\mathrm{m(R)RR}} = 200, \quad n = 2,$$
$$E_{\mathrm{mR(R)O}} = 260, \quad n = 2,$$
$$E_{\mathrm{mO(R)R}} = 340, \quad n = 1.$$

Redox cooperativity is built into the model by stipulating different E_m values for the same center, depending on the redox state of another center(s?). For example, the E_m of the a_3 center is stated as 600 mV when the other two centers are oxidized and 200 mV when they are reduced.

Because of the constraint of microscopic reversibility, in going from the *OOO* to the *RRR* state,

$$2 \cdot E_{\mathrm{mROO}} + 2 \cdot E_{\mathrm{mR(R)O}} + E_{\mathrm{mRR(R)}} = 2 \cdot E_{\mathrm{mOOR}} + E_{\mathrm{mO(R)R}} + 2 \cdot E_{\mathrm{m(R)RR}} = 1200 + 520 + E_{\mathrm{mRR(R)}} = 2 \cdot E_{\mathrm{mOOR}} + 340 + 400. \quad (18)$$

A reasonable first guess for the $E_{\mathrm{mRR(R)}}$ ($n = 1$) is 200 mV, which fixes E_{mOOR} ($n = 2$) at 590 mV. The best way to ensure consistency with microscopic reversibility during the fitting process is to attribute a standard chemical potential to each redox species as described above. For the present model, the relevant states are as follows (standard chemical potential in mV relative to *OOO* shown in parentheses): *OOO* (0), *ROO* (1,200), *OOR* (1,180), *OrR* (1,520), *RRO* (1,720), and *RrR* (1,920). The other values needed to complete this test model were arrived at in a similar way.

With this test model, a turnaround in the titration of heme a_3 is seen (Fig. 5, *top*). The voltage-dependent concentrations for each of the seven reduced species in this model are shown in the bottom panel. The equations used for testing this model against the experimental data were similar to the ones described above for the three-electron, two-center model using *OOO* as the reference state.

$$ORO = OOO \cdot 10\hat{}((E_{\mathrm{mORO}} - E)/30), \quad (19)$$
$$ROO = OOO \cdot 10\hat{}((E_{\mathrm{mROO}} - E)/30), \quad (20)$$
$$OOR = OOO \cdot 10\hat{}((E_{\mathrm{mOOR}} - E)/30), \quad (21)$$

TABLE 1 **Fitted E_m values for the single three-site model**

	mV	*n*
E_m relative to *OOO**		
EROO	600	2
EOOR	624	2
EORO	400	2
EORR	508	3
ERRO	428	4
EROR	400	4
ERRR	350	5
Single site E_m's		
ER(R)O	256	2
E(R)RO	456	2
EO(R)R	276	1
EOR(R)	724	1
ERO(R)	200	2
E(R)OR	176	2
ERR(R)	38	1
ER(R)R	150	1
E(R)RR	113	2

* Defined as the ambient redox potential at which the equilibrium concentration of the state equals that of state 000.

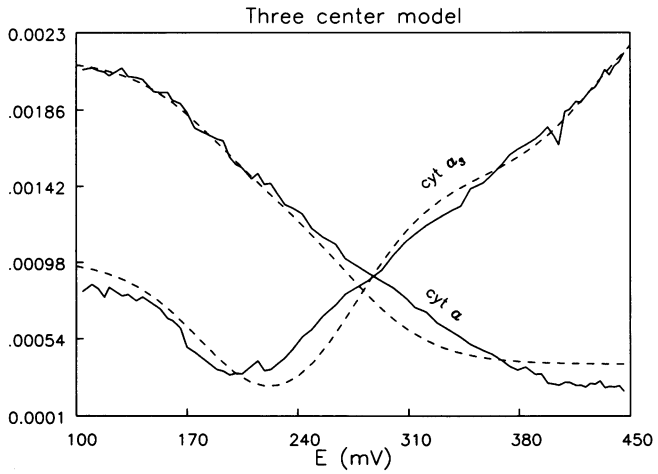

FIGURE 6 Use of equations describing the single five-electron, three-site model shown in Fig. 4 to fit experimental titration data obtained from a potentiometric titration of cytochrome aa_3. The experimental titration data (*solid lines*) are described in the legend to Fig. 3. The simulated data (*dashed lines*) were obtained by optimization of the E_m's in Eq. 29 (*frapa*3) for cytochrome *a*, and in Eq. 30 (*fra*3*exf*) for cytochrome a_3.

TABLE 2 Equations used for the voltage-independent two three-center systems model*

$$ROOU = OOOU \cdot 10\hat{}((EROOU - E)/30) \qquad ROOC = OOOC \cdot 10\hat{}((EROOC - E)/30)$$
$$OrOU = OOOU \cdot 10\hat{}((EOROU - E)/60) \qquad OROC = OOOC \cdot 10\hat{}((EOROC - E)/30)$$
$$OORU = OOOU \cdot 10\hat{}((EOORU - E)/30) \qquad OORC = OOOC \cdot 10\hat{}((EOORC - E)/30)$$
$$RrOU = OOOU \cdot 10\hat{}((ERROU - E)/20) \qquad RROC = OOOC \cdot 10\hat{}((ERROC - E)/15)$$
$$OrRU = OOOU \cdot 10\hat{}((EORRU - E)/20) \qquad ORRC = OOOC \cdot 10\hat{}((EORRC - E)/15)$$
$$RORU = OOOU \cdot 10\hat{}((ERORU - E)/15) \qquad RORC = OOOC \cdot 10\hat{}((ERORC - E)/15)$$
$$RrRU = OOOU \cdot 10\hat{}((ERRRU - E)/12) \qquad RRRC = OOOC \cdot 10\hat{}((ERRRC - E)/10)$$

$$OOOU = TU/(1 + 10\hat{}((EROOU - E)/30) + 10\hat{}((EOROU - E)/60 + 10\hat{}((EOORU - E)/30) + 10\hat{}((ERROU - E)/20) + 10\hat{}((EORRU - E)/20) + 10\hat{}((ERORU - E)/15) + 10\hat{}((ERRRU - E)/12))$$
$$OOOC = TC/(1 + 10\hat{}((EROOC - E)/30) + 10\hat{}((EOROC - E)/30) + 10\hat{}((EOORC - E)/30) + 10\hat{}((ERROC - E)/15 + 10\hat{}((EORRC - E)/15) + 10\hat{}((ERORC - E)/15 + 10\hat{}((ERRRC - E)/10))$$
$$fra = OROU + OROC + RROU + RROC + ORRU + ORRC + RRRU + RRRC$$
$$fra3 = ROOU + ROOC + RROU + RROC + RORU + RORC + RRRU + RRRC$$
$$frapa3 = fra + P \cdot fra3 + da$$
$$fra3exf = ex \cdot (ROOU = ROOC) + RROU + RROC + RORU + RORC + RRRU + RRRC + FCN/(1 + 10\hat{}((430 - E)/60) + da3$$

* Note: Because TC and TU were taken as independent, TC/TU was not a function of E. C and U were not allowed to equilibrate.

$$RRO = OOO \cdot 10\hat{}((E_{mRRO} - E)/15), \quad (22)$$
$$OrR = OOO \cdot 10\hat{}((E_{mORR} - E)/20), \quad (23)$$
$$ROR = OOO \cdot 10\hat{}((E_{mROR} - E)/15), \quad (24)$$
$$RrR = OOO \cdot 10\hat{}((E_{mRRR} - E)/12), \quad (25)$$
$$OOO = T/(1 + 10\hat{}((E_{mORO} - E)/30) + 10\hat{}((E_{mROO} - E)/30) + 10\hat{}((E_{mOOR} - E)/30) + 10\hat{}((E_{mRRO} - E)/15) + 10\hat{}((E_{mORR} - E)/20) + 10\hat{}((E_{mROR} - E)/15) + 10\hat{}((E_{mRRR} - E)/12)), \quad (26)$$
$$fra = ORO + ORR + RRO + RRR, \quad (27)$$
$$fra3 = ROO + ROR + RRO + RRR, \quad (28)$$
$$frapa3 = fra + p \cdot fra3 + da, \quad (29)$$
$$fra3exf = ex \cdot ROO + RRO + ROR + RRR + FCN/(1 + 10\hat{}((430 - E)/60)) + da3. \quad (30)$$

The fitted values for the E_m's linking each reduced state to the fully oxidized state and for each of the individual redox steps are shown in Table 1. The results of fitting the functions *frapa3* and *fra3exf* to the actual titration data are shown in Fig. 6. Although not perfect, the agreement between the predictions of this model and actual data shows an improvement over that seen for the three-electron, two-site model (Fig. 3). However, the poor agreement, especially in the voltage region above 200 mV, argues against this being a correct model to account for the titration. The titration in this region is dominated by the conversion of species *ROO* and *OrR* (*cf.* Fig. 5). These two components are the oxidized and reduced members of a one-electron couple with an effective E_m of 324 mV. The resulting simulated titration curve is obviously too steep in relation to the data that are being fitted.

The steepness of the titration curve for heme a_3 in the region where *ROO* is being converted to *OrR* can be decreased by using two separate three-center systems with two different E_m's (and n values) for the transitions. In one, heme a is uncoupled (i.e., $n = 1$), transition from *ROO* to *OrR*, and in the other, heme a functions in an electronically coupled $n = 2$ state (transition from *ROO* to *ORR*). The simplest test of such a model considers two systems, U and C, representing two different conformational states of the enzyme. Each system contains the same eight states as shown in Fig. 4. In this system, the

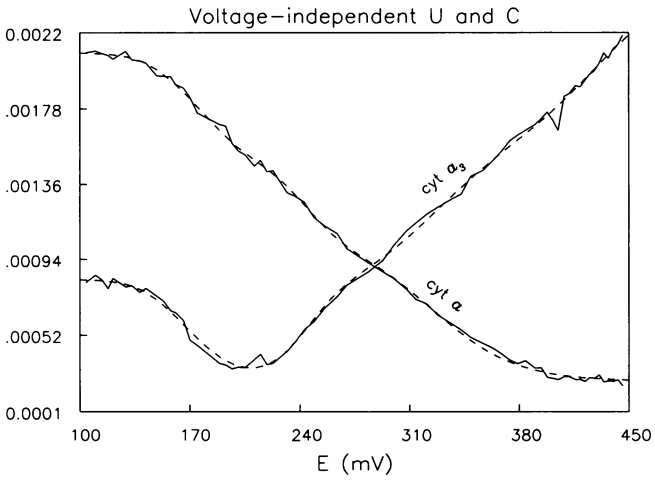

FIGURE 7 Use of equations describing two three-site systems in different conformations such that cytochrome a functions as a coupled $n = 2$ site in one conformation but as an uncoupled $n = 1$ site in the other, to fit experimental data. In this model, the two conformations were not allowed to equilibrate with each other. The equations used are described in the text and in Table 2. The experimental titration data (*solid lines*) are described in the legend to Fig. 3. The simulated data (*dashed lines*) were obtained by optimization of the E_m's in the equations "*frapa3*" for cytochrome a and "*fra3exf*" for cytochrome a_3, shown in Table 2. Other fitted parameters were as follows: TU = 0.001127, TC = 0.0007115, EX = 1.41618, P = 0.96418, FCN = 0.000888.

TABLE 3 **Fitted E_m values for voltage-independent two three-systems model**

E_m relative to *OOOU*	mV	*n*	E_m relative to *OOOC*	mV	*n*
EROOU	600	2	*EROOC*	600	2
EOROU	340	1	*EOROC*	260	2
EOORU	400	2	*EOORC*	400	2
ERROU	504	3	*ERROC*	418	4
ERORU	400	4	*ERORC*	400	4
EORRU	498	3	*EORRC*	414	4
ERRRU	370	5	*ERRRC*	342	6
			E_m's for single site reductions		
ER(R)OU	312	1	*ER(R)OC*	236	2
ERO(R)U	200	2	*ERO(R)C*	200	2
E(R)ROU	586	2	*E(R)ROC*	576	2
E(R)ORU	400	2	*E(R)ORC*	400	2
EO(R)RU	694	1	*EO(R)RC*	428	2
EOR(R)U	577	2	*EOR(R)C*	568	2
ERR(R)U	169	2	*ERR(R)C*	190	2
ER(R)RU	250	1	*ER(R)RC*	226	2
E(R)RRU	178	2	*E(R)RRC*	198	2

conversion of *ROO* to *ORR* is governed by two separate E_m's and two separate *n* values. In the U system, the conversion of *ROO* to *OrR* takes place with an effective E_m = 340 mV and *n* = 1, whereas in the other system (C), the conversion to *ORR* occurs near 260 mV with an *n* = 2. This kind of conversion that causes a simultaneous oxidation of heme a_3 and reduction of heme *a* is seen to occur in actual titrations. The fitted parameters for E_m's and *n* values obtained from the experimental data were as described above. Using the nomenclature introduced above, the equations that describe this model are shown in Table 2. The amounts of the total system in the U form and in the C form become fitted parameters (i.e., TU and TC). It should be noted that in this model, the U and C states are not allowed to equilibrate with each other.

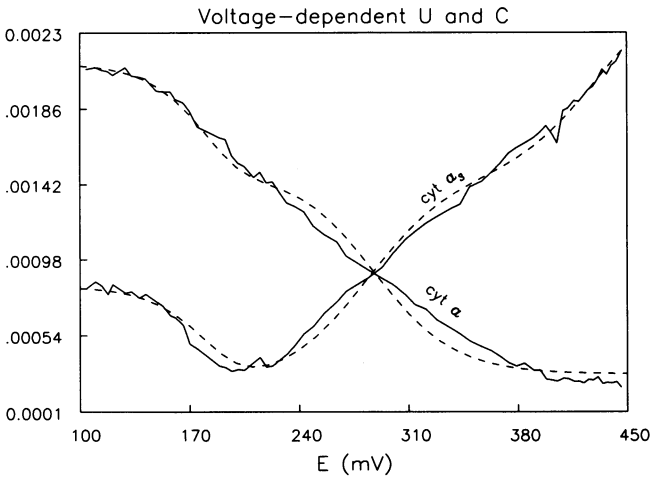

FIGURE 8 Use of equations describing a voltage-dependent equilibration of two three-center systems in different conformations such that cytochrome *a* behaves as an *n* = 1 center in one and as an *n* = 2 center in the other to fit experimental data describing the potentiometric titration of cytochrome aa_3. The equations used are described in the text (Eqs. 31–35). The experimental data (*solid lines*) are described in the legend to Fig. 3. The simulated data (*dashed lines*) were obtained by optimization of the E_m's in the equations "*frapa3*" for cytochrome *a* and "*fra3exf*" for cytochrome a_3 described in the text and in Table 2.

Fig. 7 shows the experimental and fitted curves for cytochromes *a* and a_3. The fitted E_m values used in drawing the curves are shown in Table 3. Although not perfect, Fig. 7 shows that cooperative models that take into consideration multiple redox interactions involving all of the redox centers in cytochrome *c* oxidase are able to account for the experimental observations. The composite curves for cytochrome *a* and cytochromes a_3 shown in Fig. 7 are each representative of a sum of many individual species that rise and fall with voltage such as shown in Fig. 5.

Another and more likely view of an interactive three-center system with two conformations is that there is equilibration. The equilibration between the U and C forms in a particular redox state is accompanied by a total equilibration of the rest of the system as dictated by all of the E_m's. For this analysis, we have chosen the fully oxidized state as the one through which equilibration of the U and C systems occurs as defined by:

$$OOOC = K \cdot OOOU. \quad (31)$$

The Nernst equations that express each of the 14 reduced states as a function of the fully oxidized state are the same as shown in Table 2. The equations for the functions *fra*, *fra3*, *frapa3*, and *fra3exf* are also the same. The difference in the two models is expressed in the

TABLE 4 **Fitted E_m values for voltage-dependent two three-systems model**

E_m relative to *OOOU*	mV	*n*	E_m relative to *OOOC*	mV	*n*
EROOU	600	2	*EROOC*	600	2
EOROU	340	1	*EOROC*	260	2
EOORU	400	2	*EOORC*	400	2
ERROU	336	3	*ERROC*	216	4
ERORU	400	4	*ERORC*	400	4
EORRU	504	3	*EORRC*	412	4
ERRRU	384	5	*ERRRC*	326	6
			E_m's for single site reductions		
ER(R)OU	336	1	*ER(R)OC*	216	2
ERO(R)U	200	2	*ERO(R)C*	200	2
E(R)ROU	598	2	*E(R)ROU*	556	2
E(R)ORU	400	2	*E(R)ORC*	400	2
EO(R)RU	712	1	*EO(R)RC*	424	2
EOR(R)U	586	2	*EOR(R)C*	564	2
ERR(R)U	192	2	*ERR(R)C*	162	2
ER(R)RU	320	1	*ER(R)RC*	178	2
E(R)RRU	204	2	*E(R)RRC*	154	2

TABLE 5 **Equations used for the voltage-dependent monomer/dimer system**

$$ROOU = RrRU \cdot 10^{((E - EROOU)/20)} \qquad ROOC = RRRC \cdot 10^{((E - EROOC)/15)}$$
$$OrOU = RrRU \cdot 10^{((E - EOROU)/15)} \qquad OROC = RRRC \cdot 10^{((E - EOROC)/15)}$$
$$OORU = RrRU \cdot 10^{((E - EOORU)/20)} \qquad OORC = RRRC \cdot 10^{((E - EOORC)/15)}$$
$$RrOU = RrRU \cdot 10^{((E - ERROU)/30)} \qquad RROC = RRRC \cdot 10^{((E - ERROC)/30)}$$
$$OrRU = RrRU \cdot 10^{((E - EORRU)/30)} \qquad ORRC = RRRC \cdot 10^{((E - EORRC)/30)}$$
$$RORU = RrRU \cdot 10^{((E - ERORU)/60)} \qquad RORC = RRRC \cdot 10^{((E - ERORC)/30)}$$
$$OOOU = RrRU \cdot 10^{((E - EOOOU)/12)} \qquad OOOC = RRRC \cdot 10^{((E - EOOOC)/10)}$$

$$[\Sigma XYZU] = 1 + 10^{((E - EOROU)/15)} + 10^{((E - EROOU)/20)} + 10^{((E - EOORU)/20)} + 10^{((E - ERROU)/30)} + 10^{((E - EORRU)/30)} + 10^{((E - ERORU)/60)} + 10^{((E - EOOOU)/15)}$$
$$[\Sigma XYZC] = 1 + 10^{((E - EOROC)/15)} + 10^{((E - EROOC)/15)} + 10^{((E - EOORC)/15)} + 10^{((E - ERROC)/30)} + 10^{((E - EORRC)/30)} + 10^{((E - ERORC)/30)} + 10^{((E - EOOOC)/10)}$$

functions for $OOOU$ and $OOOC$. The expression for the total, T, of all of the different states in the two systems is:

$$T = OOOU \cdot (\Sigma XYZU) + OOOC \cdot (\Sigma XYZC), \quad (32)$$

where the ΣXYZ terms are one plus the exponential functions on the right-hand sides of the equations shown in Table 2. Using Eq. 31, Eq. 32 can be restated as:

$$T = OOOU \cdot ((\Sigma XYZU) + K \cdot (\Sigma XYZC)), \quad (33)$$

and rearranged to:

$$OOOU = T/((\Sigma XYZU) + K \cdot (\Sigma XYZC)). \quad (34)$$

The explicit function for $OOOU$ used in testing this model is:

$$\begin{aligned} OOOU = {} & T/(1 + 10^{((E_{mOrOU} - E)/60)} \\ & + 10^{((E_{mROOU} - E)/30)} + 10^{((E_{mOORU} - E)/30)} \\ & + 10^{((E_{mRrOU} - E)/20)} + 10^{((E_{mOrRU} - E)/20)} \\ & + 10^{((E_{mRORU} - E)/15)} + 10^{((E_{mRrRU} - E)/12)} \\ & + K \cdot (1 + 10^{((E_{mOROC} - E)/30)} \\ & + 10^{((E_{mROOC} - E)/30} + 10^{((E_{mOORC} - E)/30)} \\ & + 10^{(E_{mRROC} - E)/15)} + 10^{((E_{mORRC} - E)/15)} \\ & + 10^{((E_{mRORC} - E)/15)} + 10^{((E_{mRRRC} - E)/10)}). \end{aligned} \quad (35)$$

Fig. 8 shows the fits to experimental data obtained with this model. Table 4 shows the fitted values for the E_m's of all of the reduced states relative to the appropriate fully oxidized state and to the closest oxidized states. It is obvious that these fits are not very good.

Another important consideration that could have a major influence on the interactive models we are exploring here is the possibility of a monomer/dimer equilibrium. It is known that cytochrome oxidase exists in both monomer and dimer forms (Wikström et al., 1981). It is possible that the dimer may be the form in which heme a is coupled to Cu_A to produce the $n = 2$ titration we have seen and that in the monomer form, heme a is titrated as an $n = 1$ center. The association constant for this equilibrium involving the fully oxidized forms is

$$K_A = \frac{[OOOC]}{[OOOU]^2}. \quad (36)$$

Because $[OOOC]$ is proportional to the square of $[OOOU]$ and $[OOOU]$ becomes very small in the voltage range of interest, $[OOOC]$ tends to vanish. Therefore, to examine this cooperative model we used the fully reduced form as the reference state.

$$K_A = \frac{[RRRC]}{[RrRU]^2}. \quad (37)$$

It should be noted that for K_A to be independent of redox potential, $RRRC$ and $2 \cdot (RrRU)$ must be isoelectronic; their interconversion must be redox neutral. We shall assume that this is the case, which implies that in the monomer, a fourth redox center (e.g., Cu_A) undergoes a silent one-electron transition.

The total concentration of monomer enzyme in the system can be described as:

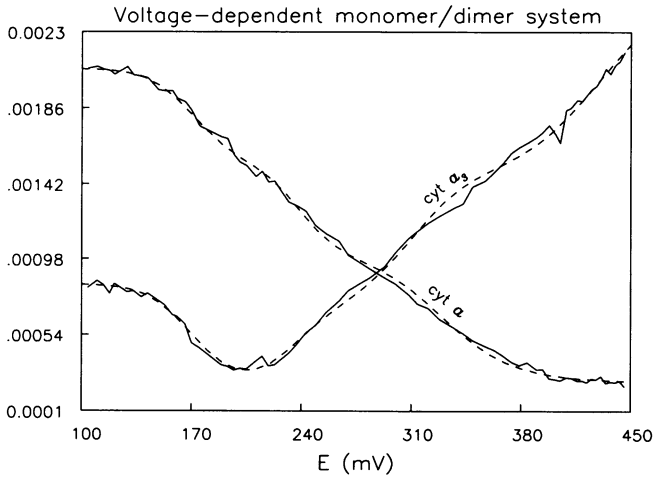

FIGURE 9 Use of equations describing a monomer/dimer equilibrium between two three-center systems where cytochrome a is coupled to another center in the dimer but is uncoupled in the monomer to fit experimental titration data obtained using cytochrome aa_3. The equations used are described in the text and in Table 5. The experimental data (*solid lines*) are described in the legend to Fig. 3. The simulated data (*dashed lines*) were obtained by optimization of the E_m's in the equations "*frapa3*" for cytochrome a and "*fra3exf*" for cytochrome a_3 described in the text and in Table 2.

TABLE 6 **Fitted E_m values for voltage-dependent monomer/dimer system**

E_m relative to *RRRU*	mV	*n*	E_m relative to *RRRC*	mV	*n*
EROOU	619	3	*EROOC*	662	4
EOROU	340	4	*EOROC*	286	4
EOORU	400	3	*EOORC*	402	4
ERROU	206	2	*ERROC*	160	2
ERORU	340	1	*ERORC*	260	2
EORRU	270	2	*EORRC*	186	2
EOOOU	388	5	*EOOOC*	354	6
			E_m's for single site reductions		
ER(R)OU	290	1	*ER(R)OC*	240	2
ERO(R)U	181	2	*ERO(R)C*	140	2
E(R)ROU	594	2	*E(R)ROC*	616	2
E(R)ORU	400	2	*E(R)ORC*	400	2
EO(R)RU	600	1	*EO(R)RC*	474	2
EOR(R)U	530	2	*EOR(R)C*	590	2
ERR(R)U	206	2	*ERR(R)C*	160	2
ER(R)RU	340	1	*ER(R)RC*	260	2
E(R)RRU	270	2	*E(R)RRC*	186	2

$$T = [RrRU] \cdot [\Sigma XYZU] + 2 \cdot [RRRC] \cdot [\Sigma XYZC]. \quad (38)$$

Using Eq. 37,

$$T = [RrRU] \cdot [\Sigma XYZU] + 2 \cdot [RrRU]^2 \cdot K_A \cdot [\Sigma XYZC]. \quad (39)$$

This is a quadratic equation from which we derive,

$$[RrRU] = 2 \cdot T/([\Sigma XYZU] + \sqrt{[\Sigma XYZ]^2 + 8 \cdot T \cdot K_A \cdot [\Sigma XYZC]}). \quad (40)$$

This equation is in a different form that avoids problems due to subtractive roundoff in the fitting process. The equations for *fra*, *fra3*, *fra3exf*, and *frapa3* are the same as shown in Table 2.

The other equations needed for testing the model are shown in Table 5. The results of fitting this model to the experimental data are shown in Fig. 9. Fitted values for the E_m's are shown in Table 6. The fits obtained with this model are quite good.

Four-site models

In the three center models, Cu_A was not treated as a separate redox center. In the coupled or C system, Cu_A was considered to be electronically linked to heme *a*, so that the two centers titrated together as an $n = 2$ unit. In the U system, Cu_A was considered to be electronically isolated from the other centers. In our model, its titration did not influence the optical spectra nor the E_m's of the other centers. If we treat Cu_A as a separate center that can interact with the other centers, a four-site model is obtained that allows greater freedom in fitting the model to data. As before, heme a_3 is considered to be coupled to Cu_B, forming an $n = 2$ center. The fourth center, *X*, can

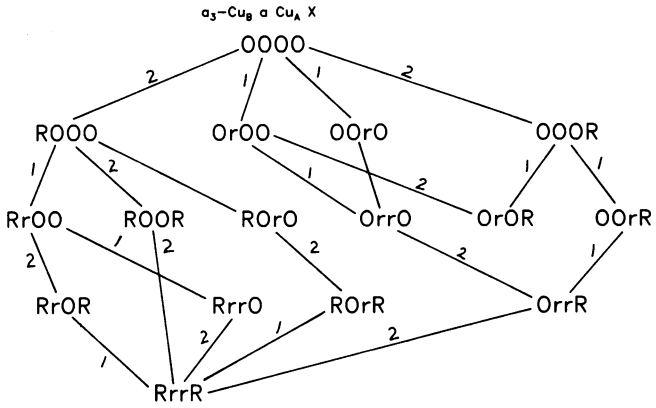

FIGURE 10 A four redox center model. The far left site represents a coupled cytochrome a_3-Cu_B center. The next sites to the right represent cytochrome *a*, Cu_A, and *X*, respectively. Not all pathways are shown. The numbers shown for each path represent *n* values.

be either $n = 1$ or $n = 2$ so that the model can involve five or six electrons. We have explored a four-center model with the *X* center as $n = 2$. It is not implied nor required that the *X* center be $n = 2$.

There are 32 possible routes to go from state *OOOO* to *RRRR* if each step results in the reduction of one of the four oxidized centers. In Fig. 10, we show a four-center

TABLE 7 **Equations used for the four-center model**

$$ROOO = OOOO \cdot 10^{((EROOO - E)/30)}$$
$$OrOO = OOOO \cdot 10^{((EOROO - E)/60)}$$
$$OOrO = OOOO \cdot 10^{((EOORO - E)/60)}$$
$$OOOR = OOOO \cdot 10^{((EOOOR - E)/30)}$$
$$RrOO = OOOO \cdot 10^{((ERROO - E)/20)}$$
$$ROOR = OOOO \cdot 10^{((EROOR - E)/15)}$$
$$ROrO = OOOO \cdot 10^{((ERORO - E)/20)}$$
$$OrrO = OOOO \cdot 10^{((EORRO - E)/30)}$$
$$OrOR = OOOO \cdot 10^{((EOROR - E)/20)}$$
$$OOrR = OOOO \cdot 10^{((EOORR - E)/20)}$$
$$RrOR = OOOO \cdot 10^{((ERROR - E)/12)}$$
$$RrrO = OOOO \cdot 10^{((ERRRO - E)/15)}$$
$$ROrR = OOOO \cdot 10^{((ERORR - E)/12)}$$
$$OrrR = OOOO \cdot 10^{((EORRR - E)/15)}$$
$$RrrR = OOOO \cdot 10^{((ERRRR - E)/10)}$$

$$OOOO = T/(1 + 10^{((EROOO - E)/30)} + 10^{((EOROO - E)/60)} + 10^{((EOORO - E)/60)} + 10^{((EOOOR - E)/30)} + 10^{((ERROO - E)/20)} + 10^{((EROOR - E)/15)} + 10^{((ERORO - E)/20)} + 10^{((EORRO - E)/30)} + 10^{((EOROR - E)/20)} + 10^{((EOORR - E)/20)} + 10^{((ERROR - E)/12)} + 10^{((ERRRO - E)/15)} + 10^{((ERORR - E)/12)} + 10^{((EORRR - E)/15)} + 10^{((ERRRR - E)10)})$$

$$fra = OROO + RROO + ORRO + OROR + RROR + RRRO + ORRR + RRRR$$
$$fra3 = ROOO + RROO + ROOR + RORO + RROR + RRRO + RORR + RRRR$$
$$frapa3 = fra + p \cdot fra3 + da$$
$$fra3exf = ex \cdot ROOO + RROO + ROOR + RORO + RROR + RRRO + RORR + RRRR + FCN/(1 + 10^{((430 - E)/60)}) + da3$$

model that displays both $n = 1$ (uncoupled) and $n = 2$ (coupled) reductions of heme *a* as well as the reciprocal relationship between the reduction of heme *a* and the oxidation of heme a_3 and also the turnaround phenomenon seen in the titration of heme a_3. The equations used to describe this model are shown in Table 7.

This model did provide for a reasonable fit to the experimental data (Fig. 11). The fitted values for the E_m's are shown in Table 8.

TABLE 8 **Fitted E_m values for four-center model**

E_m relative to *OOOO*	mV	*n*
EROOO	596	2
EOROO	340	1
EOORO	260	1
EOOOR	610	2
ERROO	500	3
EROOR	404	4
ERORO	460	3
EORRO	260	2
EOROR	490	3
EOORR	494	3
ERROR	378	5
ERRRO	396	4
ERORR	360	5
EORRR	422	4
ERRRR	335	6
E_m's for single site reductions		
ER(R)OO	308	1
EROO(R)	212	2
ERO(R)O	188	1
EOR(R)O	180	1
EO(R)RO	260	1
EO(R)OR	250	1
EORO(R)	565	2
EOO(R)R	262	1
ERRO(R)	195	2
ERR(R)O	84	1
EROR(R)	210	2
EORR(R)	584	2
EO(R)RR	206	1
ERR(R)R	120	1
ERRR(R)	213	2
ER(R)RR	210	1
E(R)RRR	161	2

SUMMARY

Ideas about the thermodynamic properties of cytochrome aa_3 that have prevailed during the past several decades have neglected the potential complexity of redox and conformational interactions that can influence its behavior. Prompted by experimental observations that are not explainable by the earlier incomplete redox models of this enzyme, a more complete analysis of complex redox interactions was undertaken. In this article, we present new approaches that can be used to model any set of experimental data obtained with this or any other cooperative enzyme. The successful fitting of data by a particular model does not prove that the model is correct but is a requirement for the continued use of such a model. In part 4, we have elaborated various models for redox cooperativity in cytochrome oxidase and compared their predictions with experimental titrations of the enzyme. Some of these models, notably the two-center, two-electron models, were falsified by the data. We also showed that models with weak redox cooperativity cannot account for experimental redox titrations of cytochrome oxidase. To demonstrate that strong redox cooperativity can account for the data, we produced competent three- and four-center models. Although Occam's razor might suggest that the equilibrated two conformation, three-center system is correct, we believe it is premature to accept this model. More experimentation and the use of the kind of modeling described here are required before confidence can be based on one particular model. The main value of the modeling approach is that it reveals possible kinds of interactions that may be occurring and therefore may be important in understanding how electron flow is coupled to proton pumping. At the present time, we do not know how this is accomplished.

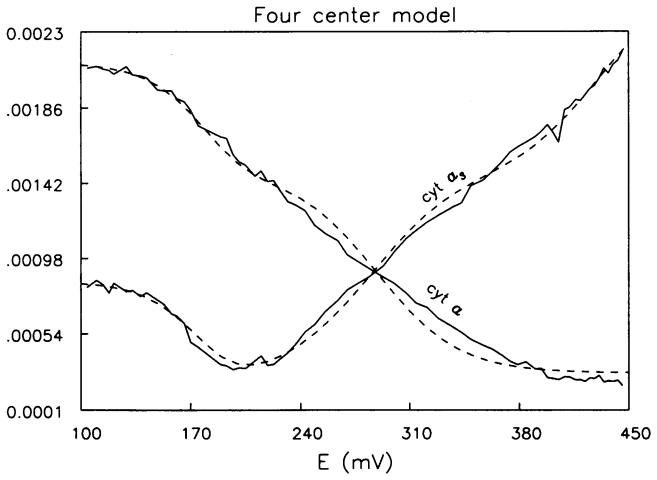

FIGURE 11 Use of equations describing the four-center model shown in Fig. 10 to fit experimental data for the titrations of cytochromes *a* and a_3. The experimental data (*solid lines*) are described in the legend to Fig. 3. The equations used are described in the text and Table 7. The simulated data (*dashed lines*) were obtained by optimization of the E_m's in the equations "*frapa3*" for cytochrome *a* and "*fra3exf*" for cytochrome a_3 described in Table 7.

We are grateful to Richard I. Shrager for his help in applying the SVD procedure to the analysis of the redox behavior of cytochrome oxidase.

H. V. Westerhoff was supported by the Netherlands Organization for Scientific Research (NWO).

Received for publication 11 November 1991 and in final form 3 August 1992.

REFERENCES

Baker, G. M., M. Noguchi, and G. Palmer. 1987. The reaction of cytochrome oxidase with cyanide. *J. Biol. Chem.* 262:595–604.

Bombelka, E., R.-W. Richter, A. Stroh, and B. Kadenback. 1986. Analysis of the Cu, Fe, and Zn contents in cytochrome *c* oxidase from different species and tissues by proton-induced x-ray emission (PIXE). *Biochem. Biophys. Res. Commun.* 140:1007–1014.

Brunori, M., G. Antonini, F. Malatesta, P. Sarti, and M. T. Wilson. 1988. Structure and function of cytochrome oxidase: a second look. *Adv. Inorg. Biochem.* 7:93–153.

Caughey, W. S., W. J. Wallace, J. A. Volpe, and S. Yoshikawa. 1976. Cytochrome *c* oxidase. *In* The Enzymes. P. D. Boyer, editor. Vol. XIII. Academic Press, New York. 299–344.

Di Cera, E. 1990. Thermodynamics of local linkage effects: contracted partition functions and the analysis of site-specific energetics. *Biophys. Chem.* 37:147–164.

Einarsdóttir, O., and W. S. Caughey. 1984. Zinc is a constituent of bovine heart cytochrome *c* oxidase preparations. *Biochem. Biophys. Res. Commun.* 124:836–842.

Einarsdóttir, O., and W. S. Caughey. 1985*a*. Possible role for adventitious copper, zinc, and magnesium in bovine heart cytochrome *c* oxidase. *Fed. Proc.* 44:1780.

Einarsdóttir, O., and W. S. Caughey. 1985*b*. Bovine heart cytochrome *c* oxidase preparations contain high affinity binding sites for magnesium as well as for zinc, copper, and heme iron. *Biochem. Biophys. Res. Commun.* 129:840–847.

Einarsdóttir, O., M. G. Choc, S. Weldon, and W. S. Caughey. 1988. The site and mechanism of dioxygen reduction in bovine heart cytochrome *c* oxidase. *J. Biol. Chem.* 263:13641–13654.

Hendler, R. W. 1991. Can ferricyanide oxidize carbon monoxide-liganded cytochrome a_3? *J. Bioenerg. Biomembr.* 23:805–817.

Hendler, R. W., and G. S. Sidhu. 1988. A new high potential redox transition for cytochrome aa_3. *Biophys. J.* 54:121–133.

Hendler, R. W., K. V. Subba Reddy, R. I. Shrager, and W. S. Caughey. 1986. Analysis of the spectra and redox properties of pure cytochrome aa_3. *Biophys. J.* 49:717–729.

Hendler, R. W., G. S. Sidhu, and K. Pardhasaradhi. 1990. High voltage properties of cytochrome *c* oxidase. *Biophys. J. 58*:897–967.

Hendler, R. W., G. S. Sidhu, and K. Pardhasaradhi. 1990. High voltage properties of cytochrome *c* oxidase. *Biophys. J.* 58:957–967.

Hill, T. L. 1985. Cooperativity Theory in Biochemistry. *Academic Press,* New York. 454 pp.

Horie, S., and M. Morrison. 1963. Cytochrome *c* oxidase components. III. Spectral properties of cytochromes *a* and a_3. *J. Biol. Chem.* 238:2859–2865.

Kamp, F., R. D. Astumian, and H. V. Westerhoff. 1988. Coupling of vectorial proton flow to a biochemical reaction by local electric interactions. *Proc. Natl. Acad. Sci. USA.* 85:3792–3796.

Kojima, N., and G. Palmer. 1983. Further characterization of the potentiometric behavior of cytochrome oxidase. Cytochrome *a* stays low spin during oxidation and reduction. *J. Biol. Chem.* 258:14908–14913.

Kroneck, P. M. H., W. E. Antholine, J. Riester, and W. G. Zumft. 1988. The cupric site in nitrous oxide reductase contains a mixed-valence [Cu(II)-, Cu(I)] binuclear center: a multifrequency electron paramagnetic resonance investigation. *FEBS (Fed. Eur. Biochem. Soc.) Lett.* 242:70–74.

Kroneck, P. M. H., W. E. Antholine, D. H. W. Kastrau, G. Buse, G. C. M. Steffens, and W. G. Zumft. 1990. Multifrequency EPR evidence for a bimetallic center at the Cu_A site in cytochrome *c* oxidase. *FEBS (Fed. Eur. Biochem. Soc.) Lett.* 268:274–276.

Leigh, J. S., D. F. Wilson, C. S. Owen, and T. E. King. 1974. Heme–heme interaction in cytochrome *c* oxidase: the cooperativity of the hemes of cytochrome *c* oxidase as evidenced in the reaction with CO. *Arch. Biochem. Biophys.* 160:476–486.

Malmström, B. G. 1974. Cytochrome *c* oxidase: some current biochemical and biophysical problems. *Q. Rev. Biophys.* 6:389–431.

Nicholls, P., and V. Hildebrandt. 1978. Binding of ligands and spectral shifts in cytochrome *c* oxidase. *Biochem. J.* 173:65–72.

Nicholls, P., and C. Petersen. 1974. Haem-haem interactions in cytochrome aa_3 during the anaerobic-aerobic transition. *Biochim. Biophys. Acta.* 357:462–467.

Nicholls, P., and J. M. Wrigglesworth. 1989. Routes of cytochrome a_3 reduction: the neoclassical model revisited. *Ann. N. Y. Acad. Sci.* 550:59–67.

Okunuki, K. B., B. Hagihara, I. Sekuzu, and T. Horie. 1957. Studies on cytochrome oxidase. *Proc. Int. Symp. Enzyme Chem.* Tokyo and Kyoto, Maruzen, Tokyo. 264.

Pardhasaradhi, K., B. Ludwig, and R. W. Hendler. 1991. Potentiometric and spectral studies with the two-subunit cytochrome aa_3 from *Paracoccus denitrificans:* comparison with the 13-subunit beef heart enzyme. *Biophys. J.* 60:408–414.

Ray, G. B., R. A. Copeland, C. P. Lee, and T. G. Spiro. 1990. Resonance Raman evidence for low-spin Fe^{2+} heme a_3 in energized cytochrome *c* oxidase: implications for the inhibition of O_2 reduction. *Biochemistry* 29:3208–3213.

Reddy, K. V. S., R. W. Hendler, and B. Bunow. 1986. Complete analysis of the cytochrome components of beef heart mitochondria in terms of spectra and redox properties: cytochrome aa_3. *Biophys. J.* 49:705–715.

Sherman, D., S. Kotake, N. Ishibe, and R. A. Copeland. 1991. Resolution of the electronic transitions of cytochrome *c* oxidase: evidence for two conformational states of ferrous cytochrome *a. Proc. Natl. Acad. Sci. USA.* 88:4265–4269.

Shrager, R. I., and R. W. Hendler. 1982. Titration of individual components in a mixture with resolution of difference spectra, pK's, and redox transitions. *Anal. Chem.* 54:1147–1152.

Shrager, R. I., and R. W. Hendler. 1986. Processing and analysis of potentiometric data. *Biophys. J.* 49:687–691.

Sidhu, G. S., and R. W. Hendler. 1990. Characterization of two low E_m forms of cytochrome a_3 and their carbon monoxide complexes in mammalian cytochrome *c* oxidase. *Biophys J.* 57:1125–1140

Steffens, G. C. M., and G. Buse. 1988. Preliminary results of anaerobic titrations of bovine heart cytochrome *c* oxidase indicate the presence of five redox active metal centers. *EBEC Reports V:*100.

Steffens, G. C. M., R. Biewald, and G. Buse. 1987. Cytochrome *c* oxidase is a three-copper, two-heme-A protein. *Eur. J. Biochem.* 164:295–300.

Tiesjema, R. H., A. O. Muijsers, and B. F. Van Gelder. 1973. Biochemical and biophysical studies on cytochrome *c* oxidase. X. Spectral and potentiometric properties of the hemes and coppers. *Biochim. Biophys. Acta.* 305:19–28.

Tsudzuki, T., and D. F. Wilson. 1971. The oxidation-reduction potentials of the hemes and copper of cytochrome oxidase from beef heart. *Arch. Biochem. Biophys.* 145:149–154.

Vanneste, W. H. 1966. The stoichiometry and absorption spectra of components *a* and a_3 in cytochrome *c* oxidase. *Biochemistry.* 5:838–848.

Walz, D. 1979. Thermodynamics of oxidation-reduction reactions and its application to bioenergetics. *Biochim. Biophys. Acta.* 505:279–253.

Westerhoff, H. V., and K. van Dam. 1987. Thermodynamics and Control of Biological Free-Energy Transduction. Elsevier, Amsterdam, The Netherlands.

Wikström, M. K. 1987. Insight into the mechanism of cellular respiration from its partial reversal in mitochondria. *Chem. Scr.* 27B:53–58.

Wikström, M. K. 1988. Mechanism of cell respiration: properties of individual reaction steps in the catalysis of dioxygen reduction by cytochrome oxidase. *Chem. Scr.* 28A:71–74.

Wikström, M. K., H. J. Harmon, W. J. Ingledew, and B. Chance. 1976. A re-evaluation of the spectral, potentiometric and energy-linked properties of cytochrome *c* oxidase in mitochondria. *FEBS (Fed. Eur. Biochem. Soc.) Lett.* 65:259–276.

Wikström, M. K., K. Krab, and M. Saraste. 1981. Cytochrome oxidase. A synthesis. Academic Press, New York. 198 pp.

Wilson, D. F., and P. L. Dutton. 1970. The oxidation-reduction potentials of cytochromes *a* and a_3 in intact rat liver mitochondria. *Arch. Biochem. Biophys.* 136:583–584.

Wilson, D. F., and J. S. Leigh. 1974. Heme–heme interaction between the cytochromes of the cytochromes of the mitochondrial respiratory chain. *Ann. N. Y. Acad. Sci.* 227:630–635.

Wilson, D. F., J. G. Lindsay, and E. S. Brocklehurst. 1972. Heme–heme interaction in cytochrome oxidase. *Biochim. Biophys. Acta.* 256:277–286.

Wrigglesworth, J. M., J. Elsden, A. Chapman, N. Van der Water, and M. F. Grahn. 1988. Activation by reduction of the resting form of cytochrome *c* oxidase: tests of different models and evidence for the involvement of Cu_B. *Biochim. Biophys. Acta.* 936:452–464.

Yonetani, T. 1960*a*. Studies on cytochrome oxidase. I. Absolute and difference absorption spectra. *J. Biol. Chem.* 235:845–852.

Yonetani, T. 1960*b*. Studies on cytochrome oxidase. II. Steady state properties. *J. Biol. Chem.* 235:3138–3143.

Yoshikawa, S., and W. S. Caughey. 1982. Heart cytochrome *c* oxidase. An infrared study of effects of oxidation state on carbon monoxide binding. *J. Biol. Chem.* 257:412–420.

Yoshikawa, S., and W. S. Caughey. 1992. Infrared evidence of azide binding to iron, copper, and non-metal sites in heart cytochrome *c* oxidase. *J. Biol. Chem.* 267:9757–9766.

Yoshikawa, S., D. H. O'Keefe, and W. S. Caughey. 1985. Investigations of cyanide as an infrared probe of hemeprotein ligand binding sites. *J. Biol. Chem.* 260:3518–3528.